Parallel Polyadenine Duplex Formation at Low pH Facilitates DNA Conjugation onto Gold Nanoparticles

by
Zhicheng Huang

A thesis
presented to the University of Waterloo
in fulfillment of the
thesis requirement for the degree of
Master of Science
in
Chemistry (Nanotechnology)

Waterloo, Ontario, Canada, 2017

Author's Declaration

I hereby declare that I am the sole author of this thesis. This is a true copy of the thesis, including any required final revisions, as accepted by my examiners.

I understand that my thesis may be made electronically available to the public.

Abstract

DNA-functionalized gold nanoparticles (AuNPs) have been extensively used in sensing, drug delivery, and materials science. A key step is to attach DNA onto AuNPs forming a stable and functional conjugate. While the traditional salt-aging method takes a full day or longer, a recent low-pH method allows DNA conjugation to happen in a few minutes. The effect of low pH was previously attributed to protonation of adenine (A) and cytosine (C), resulting in an overall lower negative charge density on DNA which is helpful for conjugating onto citrate-capped AuNPs. However, this simple charge argument does not answer why poly-A DNA works better than poly-C DNA. In addition to protonation, at low pH, DNA rich in adenine and cytosine could form higher secondary structures (e.g. the A-motif for poly-A DNA and i-motif for poly-C DNA). We suspect that such DNA folding might also play a role in DNA conjugation to AuNPs.

In this thesis, the effect of DNA conformation at low pH is studied. Using circular dichroism (CD) spectroscopy, parallel poly-A duplex (A-motif) is detected when a poly-A segment is linked to a random DNA, a design typically used for DNA conjugation. A DNA staining dye, thiazole orange, is identified for detecting such A-motifs. We found that the A-motif structure is ideal for DNA conjugation since it exposes the terminal thiol group adjacent to the poly-A for directly reacting with the gold surface while minimizing non-specific DNA base adsorption. Keeping this in mind, the order of reagent addition was further studied. However, for non-thiolated DNA, if the A-motif structure can be formed before the DNA is mixed with AuNPs, alternatively, the sample can be acidified after mixing AuNPs and DNA to then promote A-motif formation. Our results showed that the latter method is better. By taking DNA conformation into consideration, we can also explain the less optimal performance of the C-rich DNA. The i-motif formed by poly-C DNA at low pH is less favorable for the conjugation reaction due to its unique way of folding.

Finally, the stability of poly-A and poly-G DNA in low pH also is examined due to the concerns related to DNA depurination and subsequent cleavage. An excellent stability of poly-A DNA is confirmed, while poly-G has slightly lower stability. Overall, the stability is sufficient for the low pH method for DNA attachment. This study provides new fundamental insights into a practically useful technique of conjugating DNA to AuNPs.

Acknowledgements

I would like to thank my supervisor, Prof. Juewen Liu, who constantly supports and guides me throughout the whole five terms. The learning and research experience under his supervision is quite rewarding and enjoyable for me. I greatly appreciate the help from all members of this group. In particular, I would like to thank Biwu Liu and Lingzi Ma, for their making our office a great place to share ideas and happiness. I would also like to thank my committee members, Prof. Guy Guillemette and Prof. Vivek Maheshwari for their help during my seminar and later experiments. Lastly, I would like to show my gratitude towards my parents. They are the greatest parents in the word in my mind.

Dedication

I would like to dedicate this thesis to my family for their encouragement and support.

Table of Contents

List of figures

List of tables

List of abbreviations

A	Adenine
AP	Apurinic
AuNPs	Gold nanoparticles
C	Cytosine
CD	Circular dichroism
DNA	Deoxyribonucleic acid
ds-DNA	Double-strand DNA
EB	Ethidium bromide
FAM-DNA	6-carboxyfluorescein labeled DNA
G	Guanine
LSPR	Localized surface plasmon resonance
MD	Molecular dynamic
NMR	Nuclear magnetic resonance
PAGE	Polyacrylamide gel electrophoresis
PCR	Polymerase chain reaction
RNA	Ribonucleic acid
ssDNA	Single-strand DNA
SWNT	Single-wall carbon nanotube
SGI	SYBR Green I
T	Thymine
TEM	Transmission electron microscopy
TO	Thiazole orange
UV-vis	Ultraviolet and visible

Chapter 1: Introduction

1.1 Introduction to DNA

DNA (deoxyribonucleic acid) was first proved as an important carrier for genetic information by the Avery-Macleod-McCarty experiment in the 1940s. In 1953, Watson and Crick discovered the B-form DNA, which is a right-handed helical duplex structure giving the birth to molecular biology. In the following years, more and more non-B DNA structures were discovered and studied. Beyond being a genetic information carrier, DNA is also an important biopolymer. Nowadays, DNA biopolymer has attracted significant interest for its potential applications in sensing, drug delivery, nanomaterial assembly, and cell imaging.[1-6]

1.1.1 DNA as a Biopolymer

DNA is composed of four types of deoxyribonucleotides (deoxyadenosine, deoxyguanosine, deoxythymidine, and deoxycytidine) linked by a phosphate backbone. Each deoxyribonucleotide is made of a deoxyribose sugar ring, a phosphate, and one of the four nucleobases – cytosine (C), guanine (G), adenine (A), and thymine(T). In the physiological environment, nucleobases are electrically neutral, while the phosphate backbone is negatively charged. Thus, the whole single or duplex DNA is negatively charged. However, the nucleobases can be protonated at different acidic pH values depending on their pK_a's (Figure. 1.1). For example, over fifty percent of adenines are protonated when the pH is lower than 3.5. Compared with adenine, cytosine is more easily protonated due to its higher pK_a value. Base ring nitrogen and exocyclic keto groups are often used for binding to metal ions but the exocyclic amino groups are

poor ligands since their lone-pair electron is delocalized.[7] All the bases are aromatic and can achieve pi-stacking with other bases and with the pi-electron containing surfaces such as graphene.

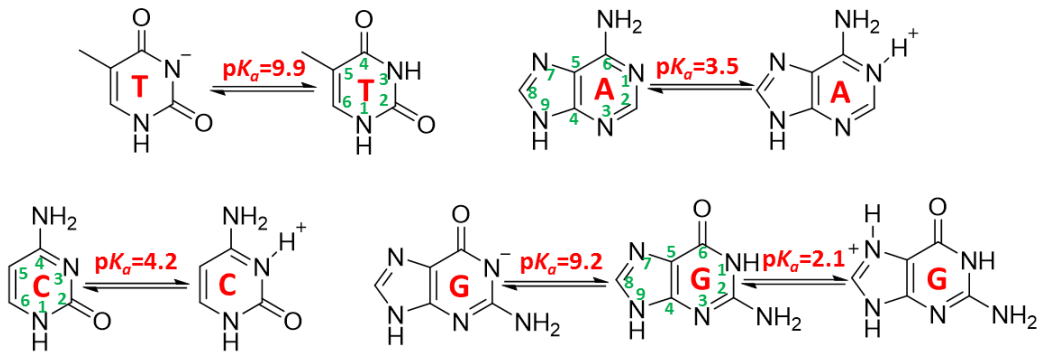

Figure 1.1 The structures of various DNA bases (Thymine, Adenine, Cytosine, Guanine) and their pK_a values. The numbering of each atom position is in green.

With the invention of DNA chemical synthesis, single-stranded (ss) DNAs with arbitrary sequences become readily available. The natural base pairing rules enable the ssDNA extensively to be used as probes for complementary nucleic acids.[8] Besides that, DNA can be immobilized on various kinds of nanomaterials of all the dimensions (1D to 3D).[9-14] These make DNA an excellent material for building artificial nanostructures in material science and nanotechnology.

1.1.2 Modified-DNA

A wide variety of modifications can be incorporated into an oligonucleotide during the time of synthesis. More than 10 different types of functional groups can be obtained from commercial sources such as phosphorylation, spacers, fluorophores, dark quenchers, and attachment linkers/chemistry. The modifications not only benefit the conjugation process between DNA and nanomaterials (e.g. thiolated DNA on AuNPs) but also offer various simple and accurate

ways to detect the changes in DNA concentrations and structures. For example, when a ssDNA is modified with a 6-carboxyfluorescein group (FAM-DNA), the amount of this ssDNA can be monitored with a fluorescence spectrophotometer under 485 nm excitation.

1.2 B-Form and Non-B DNA Conformations

Natural DNA duplexes in physiological conditions which was discovered by Watson and Crick is called B-form. B-form DNA is right-handed. In this structure, the helix makes a turn every 3.4 nm, and the distance between two neighboring base pairs is 0.34 nm. Hence, there are about 10 pairs per turn. The intertwined strands make two grooves of different widths, referred to as the major groove and the minor groove.

In contrast to the B-DNA, more non-B DNA structures were observed and folded when respective DNA sequences are incubated under certain conditions. These new structures include left-handed Z-form, hairpin, i-motif, G-quadruplex, and A-motif. When DNA, especially ssDNA, is used as the biopolymer, it cannot be B-DNA. Thus, non-B DNA conformations play a critical role in the process of conjugating DNA onto nanomaterials.[15]

1.2.1 A-motif DNA

At the very beginning of DNA research, the adenine-rich DNA was widely studied because of its ability to selectively bind small molecules. For example, coralynes can bind with two single strands poly-A oligonucleotides and a stable antiparallel duplex is formed.[16] At the same time, an adenine-rich DNA could form a parallel duplex structure with another poly-A DNA at an acidic pH. This parallel duplex structure is named A-motif. The parallel folding of poly-A DNA can be

reversibly controlled by pH changes. This feature makes the A-motif form multiple dimension pH-reversible DNA morphologies which would have potential uses in biosensors.[6] The A-motif exhibits a right-handed helical duplex with tilted protonated bases. Rich *et al.* proposed that the A-motif could be stabilized by two factors: the hydrogen bonding and the electrostatic interactions.[17] At low pH, two adenine bases are assumed to be held together by $A^{+}H\text{-}H^{+}A$ base pair. The hydrogen bond which was previously observed for a dinucleotide monophosphate can be formed between the N7 atom in one adenine with the exocyclic amino group in another adenine (Figure 1.2).[18] Meanwhile, the N1 atom in the adenine is easily protonated in acid buffers. The positively charged N1 atoms and negatively charged phosphate groups will attract each other, rendering a total of neutral charge. Therefore, at low pH, adenine-rich DNA will less repulsive to negatively charged nanomaterials (citrate capped AuNPs, Fe_3O_4 NPs, In_2O_3, *etc*.).[19]

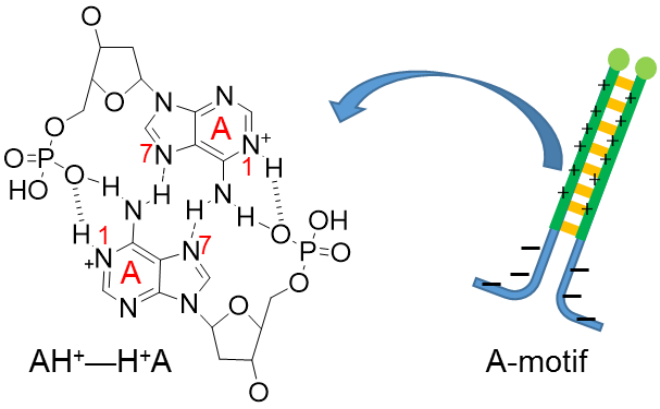

Figure 1.2 The base pairing scheme of $AH^{+}\text{-}H^{+}A$ between two adenosines at low pH. The poly-A block can form a parallel duplex, and this duplex region is positively charged. (Poly-A sequences in green and random sequence in blue)[20] (Reproduced with permission from ref. 20)

A systematic work was done to study specifically the pH conditions effects on forming the A-motif structures. As a result, the majority of the poly-A DNAs can form the A-motif structures at pH 3.0. This is important because my major work in this thesis is to study the effect of DNA

conformation on conjugating AuNPs at pH 3.0. With the increase of the pH, less adenine rich DNA are involved in the A-motif. When the pH is higher than 6.0, poly-A DNA exists as a single-stranded structure which is obvious in the gel electrophoresis (Figure 1.3).

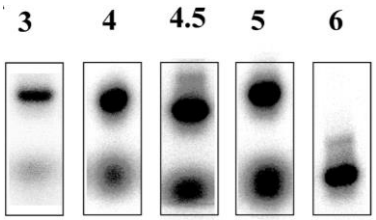

Figure 1.3 Gel electrophoresis of poly-A DNA A_{15} at different pH values.[17] (The upper bands are the parallel duplex, or the A-motif, and the low bands are the single-strand A_{15}) (Reproduced with permission from ref. 16)

1.2.2 i-motif DNA

Another well-known example is the i-motif formed by the DNA which is rich in cytosine at low pH. Due to the distinctive four-stranded DNA structure, the i-motif structures are more variable depending on the number of cytosine bases and external conditions. Different from the A-motif, i-motif bonding requires only one protonated cytosine and another ground-state cytosine (Figure 1.4). Therefore, the typical pH condition of forming i-motif is around 5.0. At the same time, the pH condition could be altered by combining the poly-C DNA and nanomaterials. For example, with the help of SWNT, i-motif can be formed at pH 8.0.[21] When conjugating the homo oligonucleotides on the AuNPs, our group found that poly-C and poly-A both have relatively higher DNA adsorption densities compared with poly-T and poly-G.[22] Comparing the roles of i-motif and A-motif in the process of conjugating DNA onto AuNPs is important for understanding parallel structure importance.

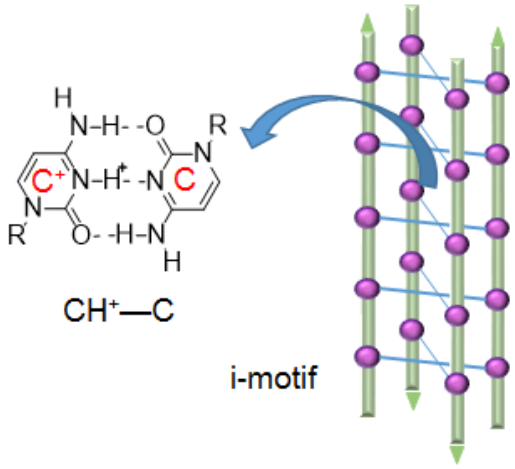

Figure 1.4 The base pairing scheme of CH^+-C between two cytosine at low pH. i-motif are four-stranded DNA structure (Cytosine).

1.3 Noble Metal Nanoparticles

Noble metal nanoparticles are much more precious than the bulk metals due to the super high specific surface area and quantum effects. The developments in the synthesis of noble metal nanoparticles with controlled morphologies have greatly extended the nanoparticles' properties.

1.3.1 Gold Nanoparticles (AuNPs)

AuNPs have fascinating catalytic, electronic, and optical properties. Citrate-capped 13 nm AuNPs were chosen as the substrate in my experiments because of its good stability, uniformity, and the easy synthesis process. AuNPs show different optical properties compared with bulk gold. For example, AuNPs appear red when their diameters are smaller than 80 nm and blue/purple when their diameters get larger (Figure 1.5 A). In some cases, the purple color may be induced by the aggregation or self-assembly of the smaller AuNPs. Different sizes of AuNPs also haves different UV-vis absorbance (Figure 1.5 B). This UV-vis absorbance spectra are usually utilized to analyze

the uniformity and stability of AuNPs. Similarly, when AuNPs were modified with other functional polymers (e.g., DNA), the changes in size also can be reflected in the UV spectrum. The ultimate reason for these phenomena is the AuNPs' geometry, i.e., surface modification, thickness, lateral size, and degree of corner truncation.[23]

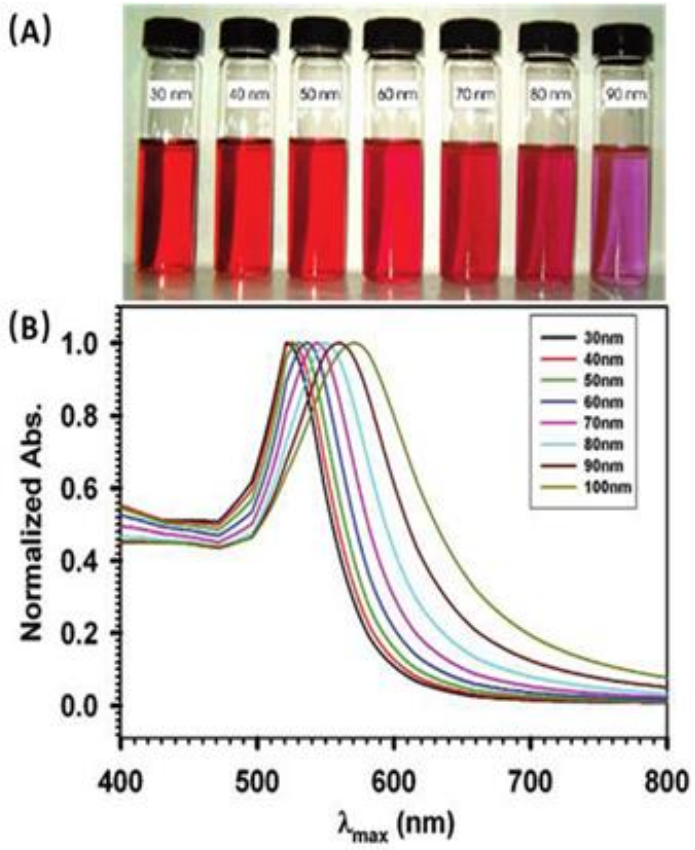

Figure 1.5 (A) The different colors of the AuNPs with diameter from 30 nm to 90 nm (from left to right). (B) The UV-vis absorption spectrums of AuNPs with different sizes.[24] (Reproduced with permission from ref. 24)

1.4 DNA-AuNPs conjugates

DNA functionalized AuNPs are well-developed and have been undergoing continuous exploration over several decades for various applications including sensing, imaging, catalysis, therapeutics, diagnostics, and drug delivery.[25-27] Large scale DNA origami and other DNA patterns provide powerful routes to self-assemble AuNPs in a programmable fashion. Short DNA sequences functionalized AuNPs conjugates are ideal probes for constructing biorecognition and transduction layers in biosensing applications. Rationally designed DNA probes can be designed to virtually detect DNA and RNA.[3, 28-30] Some DNAs with unique sequences, which are DNAzyme and DNA aptamer, even can recognize proteins, ions and small molecules.[31, 32]

1.4.1 Interactions between DNA and AuNPs

The interaction between DNA and AuNPs is an interesting biointerfacial topic with applications in analytical chemistry,[33-38] drug delivery,[39, 40] and materials science.[41-44] AuNPs have a strong inter-particle van der Waals force, and citrate-capped AuNPs used in this project are only stabilized by weak electrostatic repulsion, rendering them easily aggregated at a slightly elevated ionic strength. The interaction between non-modification DNA and AuNPs is mainly depended on the nucleobases (Figure 1.6). The relative affinities of DNA bases and AuNPs surface follow the trend A > C > G > T.[45]

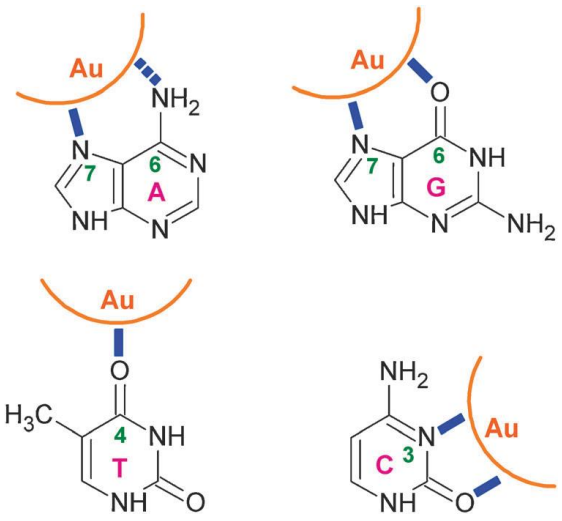

Figure 1.6 Four DNA bases adsorption on gold surface.[46] (Reproduced with permission from ref. 46)

On the other hand, in order to obtain covalent binding, thiolated DNA is the most commonly used reagent for functionalizing AuNPs due to the strong thiol-gold interaction.[47, 48] The colloidal stability of AuNPs is significantly improved upon DNA conjugation. Between the thiol group and the DNA sequence intended for hybridization, a polynucleotide spacer is often added. Historically, the Mirkin group used a poly-A spacer for many years, and this has been followed by many others. Further studies showed that a poly-A DNA binds to gold surfaces quite strongly,[49, 50] and the more weakly interacting poly-T spacers support the highest DNA loading density.[51] Regardless of the spacer sequence, in a typical conjugation reaction, thiolated DNA is mixed with AuNPs and the NaCl concentration is gradually raised to ~300 mM over a few hours to a day to achieve a stable conjugate.[52]

In 2012, we studied the adsorption of DNA by AuNPs and identified the critical role of pH,[53] allowing DNA conjugation reaction in a few minutes at pH 3.0.[54] The same method was also successfully applied to larger AuNPs,[55, 56] Au nanorods,[57] silver NPs,[58] and platinum NPs.[59] Quite

interestingly, a high density of non-thiolated DNA with a poly-A fragment can also be adsorbed at low pH.[22]

1.4.2 The Salt-Aging Method

We first describe the salt-aging process to understand the surface chemistry of DNA adsorption (Figure 1.7).[47, 52] Upon the initial mixing, only a few DNAs are adsorbed, both by the thiol group and the DNA bases. At a given ionic strength, an equilibrium is reached due to electrostatic repulsion between the adsorbed DNA and the DNA in solution. This equilibrium is shifted by raising the salt concentration to further screen the charge repulsion, allowing more DNA adsorption. Gradually, the DNA bases are displaced by the thiol groups of the newly adsorbed DNA (i.e. thiol affinity to gold is stronger than DNA base affinity), forcing each DNA to stand up. Finally, a highly stable conjugate is obtained, and the whole procedure usually requires a day or longer. In this salt-aging process, the spacer sequence (in green) does not play a critical role and it can be any nucleotide. Traditionally, a poly-A spacer was used.

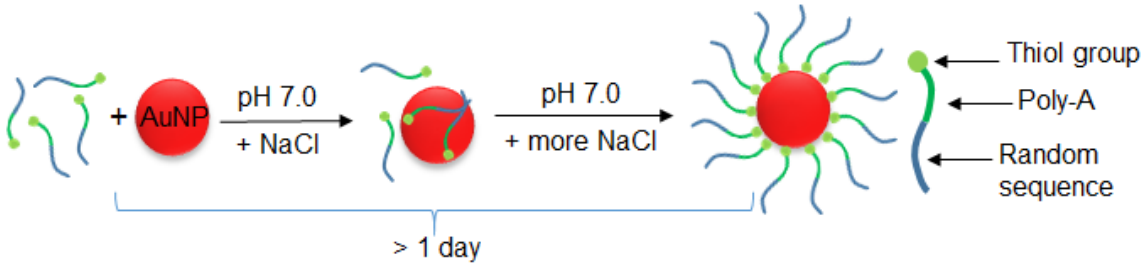

Figure 1.7 Schemes of adsorption of thiolated DNA onto AuNPs by the salt-aging method.

1.4.3 The Low-pH Method

The adsorption process of the low-pH method can save hours compared with the salt-aging process. Firstly, citrate-capped 13 nm AuNPs are mixed with DNA for 1 minute. Secondly, the

reaction solution is adjusted to pH 3.0 by citrate buffer (10 mM) and stands for 3 minutes at room temperature. Thirdly, all samples are centrifuged and washed at least three times with HEPES buffer (5 mM) pH 7.6 to remove the free DNA. (Figure 1.8)

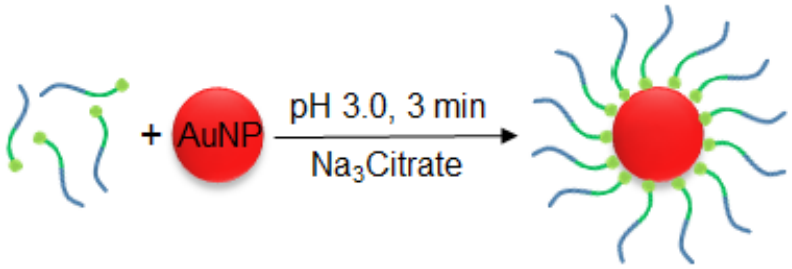

Figure 1.8 Schemes of adsorption of thiolated DNA onto AuNPs by the low-pH method.

1.5 Thesis Objective

Due to the unique properties, DNA-AuNPs conjugates have received wide interest and have been extensively studied. However, the mechanism of nonthiolated DNA, especially, the DNA with a poly-A fragment, adsorption on AuNPs surface by the low-pH method has yet to be fully understood. We used to explain the pH effect mainly based on charge. Adenine (pK_a = 3.5) can be protonated at pH 3.0, which decreases the negative charge density on DNA and facilitates DNA adsorption. However, this simple charge model cannot account for all the observations. 1) Based on the salt-aging model, DNA should first lie down on AuNPs since DNA bases can also bind to gold strongly.[47, 52] Gradually, the adsorbed DNA stands up due to displacement by the thiol group from the new incoming DNA. Introducing a positive charge to DNA bases should even promote DNA base adsorption (i.e., the thiols cannot easily replace the nucleobases). 2) More surprisingly, we achieved a high loading density of non-thiolated poly-A DNA similar to that for thiolated DNA (e.g. >60 poly-A DNA per 13 nm AuNP).[22, 60] The adsorption density of adenine even is higher than cytosine which should be more positively charged at pH 3.0. Without a thiol

group, DNA is expected to wrap around AuNPs,[61-65] which should limit its density and functionality. Therefore, other reasons must also be considered beyond simple protonation of DNA bases.

At low pH, DNA adopts different conformations beyond those based on the typical Watson-Crick base pairing, which may also affect the adsorption process. A well-known example is the i-motif formed by poly-C DNA. Poly-A DNA also can form parallel duplexes in acidic pH.[66, 67] In this thesis, we aim to understand the effect of DNA conformation at low pH and its effect on the AuNPs conjugation reaction. In particular, we focus on the poly-A parallel duplex. We also want to emphasize the parallel duplex formed by the poly-A spacer sequences. The existence of the A-motif in the spacer sequences are proved by the CD spectra and staining dye. Due to the potential depuration at low pH,[68] the stability research of adenines in the A-motif cannot be ignored.

Chapter 2: A-motif Formation and Characterization

2.1 Introduction

2.1.1 A-motif Formation

At pH 3.0, the conjugation process of DNA onto AuNPs can be completed in a few minutes.[54] In this case, a poly-A spacer is particularly useful.[60] With a pK_a of 3.5, adenine is partially protonated at pH 3.0 leading to the decrease of the negative charge density of poly-A DNA. While reduced electrostatic repulsion is certainly helpful, the goal of this work is to examine the role of DNA conformation at low pH. For example, poly-A DNA can form the AH^+-H^+A base pair by a hydrogen bond between the N7 atom in one adenosine and the exocyclic amino group in another (Figure 1.2).[67, 69] The consequence is the formation of a parallel poly-A duplex (i.e. A-motif).

With the parallel A-motif duplex in mind, two thiolated DNA can be held together by the green poly-A fragment in Figure 2.1, exposing the thiol groups. This is only possible for a parallel DNA duplex so that the two thiol groups are on the same end. A further advantage is that the poly-A duplex region (i.e., space sequence) is positively charged, while the rest of the DNA is likely to be negatively charged (unless the rest of the DNA is purely poly-A/C). This favors selective adsorption of the thiolated end due to electrostatic attraction with the negatively charged AuNPs surface. Thus, such a rigid parallel duplex can also minimize internal DNA base adsorption, and the desired final structure can form just in one step (e.g. no need for thiol displacing DNA bases). All these factors may contribute to the fast DNA adsorption at low pH. The formation of A-motif can also explain the high loading density of non-thiolated poly-A DNA.[22, 60]

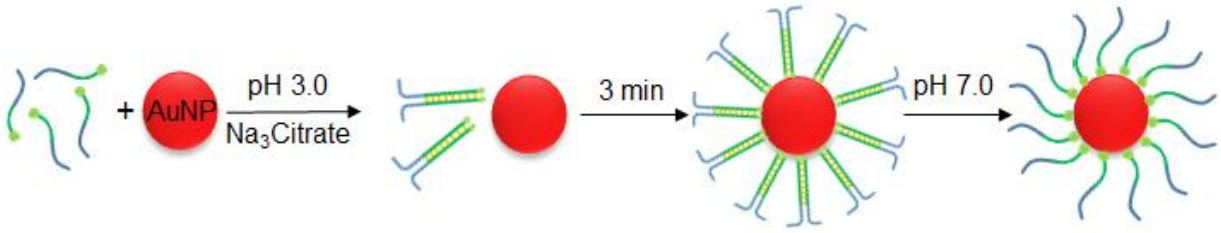

Figure 2.1 Schemes of the adsorption of thiolated DNA onto AuNPs by the low-pH method. The formation of parallel poly-A duplex is highlighted in green, leading to fully exposed thiol groups for AuNPs attachment.

2.1.2 i-motif Formation

In addition to adenine, cytosine (pKa = 4.2) can also be protonated at pH 3.0. The poly-C DNA may also form a unique structure called the 'i-motif' (Figure 1.4). The thing needs to be noted is that the i-motif structure cannot be parallel. The research on the DNA with a poly-C fragment at acidic condition also is carried out with the DNAs which have two blocks (the poly-C block and the random sequence block). This is a good control to understand the unique effect of the parallel A-motif structure.

2.1.3 Circular Dichroism (CD) Spectroscopy

The differences between the absorbance of left- and right-handed circularly polarized light by the chiral molecules is called Circular dichroism (CD) (Figure 2.2). The CD signal collected from molecules over a range of wavelength is called the CD spectrum. Particularly, CD spectrum can sensitively reflect the isomerization among distinct conformational states. The CD signal of DNA comes from the asymmetric backbone sugars and the helical arrangement of its constituents.[70] DNA CD spectroscopy research involves far UV as well as infrared light, but most

analysis is under 180-320 nm. The secondary structures of the DNA including A-motif and i-motif are good chiral response sources.

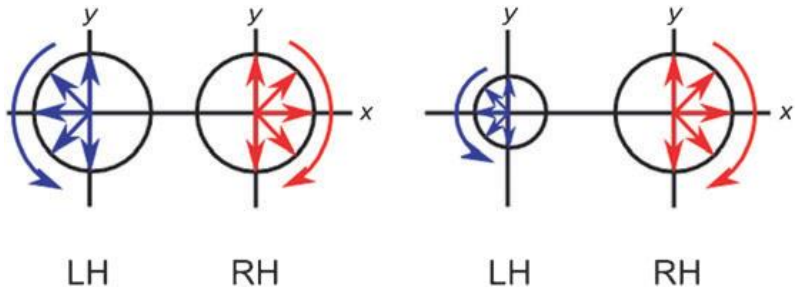

Figure 2.2 The principle of circular dichroism. The intensities of LH and RH circularly polarised light source are equal. If the sample is chiral, it will have a preference for the absorption of either LH or RH circularly polarised light (here LH).[71] (Reproduced with permission from ref. 71)

The CD spectra of both i-motif and A-motif (homo poly-A oligonucleotides) have been well studied. At pH 5.00 and 5.51, the CD spectra of cytosine rich oligonucleotides show strong positive peaks near 288 nm and negative peaks near 258 nm indicating the formation of i-motif. With the increasing pH values, both the positive and negative peaks of the CD spectrum shifts to shorter wavelengths (Figure 2.3 A). For single-stranded poly-A DNA A_{15}, there is a characteristic positive maximum CD peak at 217 nm with a shoulder at 232 nm. The spectrum of 1 µM A_{15} at pH 3.0 which shows a positive peak at 265 nm is completely different from the CD spectrum at pH 7.0. This indicates the formation of A-motif of poly-A DNA at low pH. In addition, when the DNA samples at pH 3.0 were heated over melting temperature, the peak at 265 nm totally disappears (Figure 2.3 B). In our experiments, the introduction of the conformational isomerization by poly-A/C DNA with a random sequence during the low-pH method process will be observed in the CD spectrum.

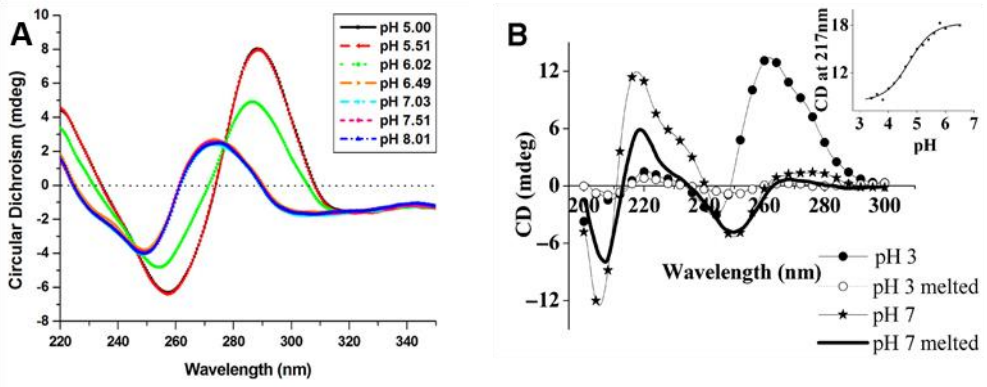

Figure 2.3 (A) CD spectra of the oligonucleotides (5′-CCC TAA CCC TAA CCC TAA CCC-3′) in various pH solutions.[72] (B) CD spectra of 1 μM A_{15} (5′-AAA AAA AAA AAA AAA-3′) at pH 3.0 and pH 7.0 recorded at both 20 ℃ and 95 ℃. Inset: CD at 217 nm of 5 μM A_{15} as a function of buffer pH.[66] (Reproduced with permission from ref. 72 and 66)

2.1.4 Fluorescent DNA Staining Dye

Fluorescent DNA staining dyes are economic materials to probe DNA structures. A trace amount of DNA can be visualized with the help of a suitable DNA staining dye. Most fluorescent DNA dyes have conjugated structures with a positive charge.[73, 74] The positive charge of the dye molecule is attractive to the negatively charged phosphate group of DNA. The fluorescence enhancement mechanisms of various dyes are different and many of them are not clear by now. The various mechanisms make DNA staining dyes have the selectivity to different DNA structures or sequences. For example, ethidium bromide (EB) is emissive when intercalated into the grooves of double-stranded DNA, but EB lack sequence specificity.[75] Another example is the indication of the i-motif by thiazole orange (TO). The TO dye was covalently modified in the cytosine rich DNA sequence. Under the same excitation wavelength, different emissions from duplex structure

(pH 7.3) and i-motif (pH 5.0) can probe the folding or unfolding of i-motif (Figure 2.4). In our work, a few DNA staining dyes were screened to study A-motif.

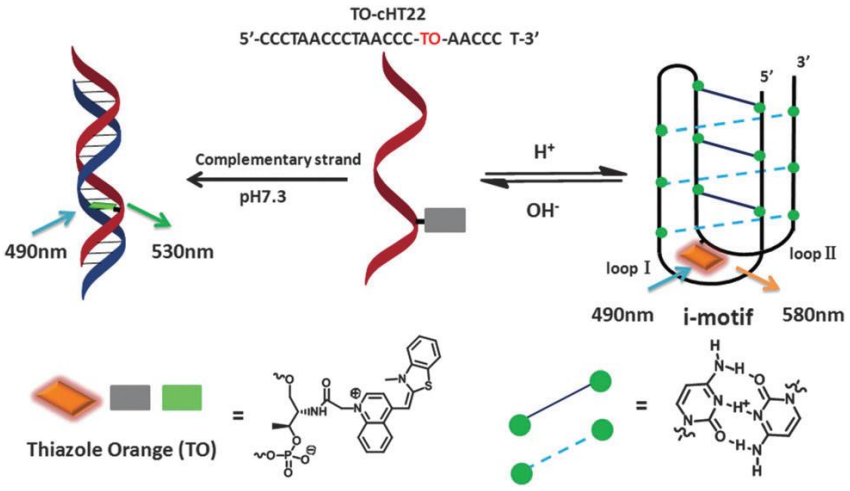

Figure 2.4 The diagram of the different emissions from TO dye in duplex and i-motif structures under 490 nm excitation light.[76] (Reproduced with permission from ref. 76)

In this chapter, our goal is to prove the existences of the A-motifs by CD spectra in the DNAs with poly-A segments at pH 3.0. At the same time, as a control, same experiments were repeated with the poly-C DNA. More than the CD spectra, which is used to characterize A-motif, a few dyes were screened to more easily indicate A-motif.

2.2 Experimental Section

2.2.1 Chemicals

All the DNA samples were from Integrated DNA Technologies (IDT, Coralville, IA). Their sequences and modifications are listed in Table 1. SYBR Green I (SGI) was from Invitrogen (Carlsbad, CA). Thiazole orange (TO) was from Sigma-Aldrich. Ethanol, sodium hydroxide, and

hydrochloric acid were from VWR (Mississauga, ON). Ethidium bromide (EB), sodium chloride, sodium citrate, and 4-(2-hydroxyethyl) piperazine-1-ethanesulfonate (HEPES) were from Mandel Scientific (Guelph, ON).

Table 2.1 A list of the DNA sequences and modifications used in this work.

DNA ID	DNA Names	Sequences and modifications (from 5′ to 3′)
1	A_0-DNA	TTCACAGATGCGT
2	A_3-DNA	TTCACAGATGCGTAAA
3	A_9-DNA	TTCACAGATGCGTAAAAAAAAA
4	A_{15}-DNA	TTCACAGATGCGTAAAAAAAAAAAAAAA
5	C_0-DNA	TTTCACAGATGCGT
6	C_3-DNA	TTTCACAGATGCGTCCC
7	C_9-DNA	TTTCACAGATGCGTCCCCCCCCC
8	C_{15}-DNA	TTTCACAGATGCGTCCCCCCCCCCCCCCC
9	A_{15}	AAAAAAAAAAAAAAA
10	T_{15}	TTTTTTTTTTTTTTT
11	G_{15}	GGGGGGGGGGGGGGG
12	C_{15}	CCCCCCCCCCCCCCC
13	A_{30}	AAAAAAAAAAAAAAAAAAAAAAAAAAAAAA
14	T_{30}	TTTTTTTTTTTTTTTTTTTTTTTTTTTTTT

2.2.2 Buffer preparation

Citrate has three pK_a values at 3.13, 4.76, and 6.40, respectively. In our experiment, pH 3.0 citrate buffer was used in all low-pH method. Citrate HCl buffers were prepared by dissolving trisodium citrate at a concentration close to 500 mM and concentrated HCl was used to adjust pH to designated values. When the pH value was table, the buffer was adjusted to the final concentration of 500 mM as the stock. Citrate pH 7.0 was prepared similarly.

HEPES has two pK_a values at 3.0 and 7.5, respectively. In our experiment, pH 7.0 HEPES buffers were prepared by dissolving HEPES at a concentration close to 500 mM and concentrated HCl/NaOH was used to adjust pH to designated values. When the pH value was table, the buffer was adjusted to the final concentration of 500 mM as the stock.

2.2.3 CD Sample Preparation and Operation Conditions

CD spectroscopy was performed in a 1 cm UV−vis quartz cuvette using a Jasco J-715 Spectrophotometer. Two 5 mM citrate buffer (pH 3.0 and 7.0) samples were measured as blanks. Each DNA sample (10 μM, 200 μL) was dissolved in 5 mM citrate buffer and was measured 10 times with the continuous scanning mode (100 nm/min) from 200 to 300 nm.

2.2.4 Fluorescence Spectrometer

Fluorescent emission spectra were recorded on a RF-5301PC spectrofluorometer (Shimadzu, Japan). Photos of the dye-DNA samples were taken under blue-light box (470 nm). All samples with 1 μM DNA, and pH=3.0 with Citrate buffer concentration 10 mM pH=7.6 with HEPES concentration 10 mM.

2.3 Results and Discussion

2.3.1 CD Spectra of A-motif

Parallel poly-A duplexes have been studied in terms of biophysical properties,[55, 77, 78] structure, and analytical applications.[6, 69, 79, 80] Most previous work focused on using pure adenine homopolymers. In our system, however, the poly-A DNA is only a fraction of the whole sequence.

In addition, there is also a fragment intended for DNA hybridization. To understand whether such DNA can form parallel duplex under our experimental conditions, circular dichroism (CD) spectroscopy was employed. The A_{15} DNA was first measured as a positive control. At pH 3.0, a characteristic positive CD peak at 268 nm was observed (Figure 2.5 A), consistent with the previous literature report of parallel poly-A duplex.[66] When the pH is raised to 7.0, the peak at 223 nm increased strongly, while the peak at 268 nm disappeared, suggesting that the A-motif structure is disrupted. We next used a random DNA (DNA 1 in Table 1) as a negative control. Its CD signal is quite weak and did not change much upon the pH drop (Figure 2.5 B).

After these control experiments, we then tested three DNA sequences (DNA 2-4); they all have the same random DNA sequence but with different lengths of the poly-A fragment. DNA with a longer poly-A fragment showed a more obvious decrease of the 223 nm peak upon the pH drop (Figure 2.5 C-E). At the same time, the peak at 268 nm is stronger with longer poly-A, suggesting a longer poly-A block can better form the A-motif structure. The CD spectral difference of DNA 4 at these two pH's (Figure 2.5 E) is not as large as that in the pure A_{15} DNA (Figure 2.5 A), although they both contained an A_{15} fragment. This is likely due to the signal from the random sequence in DNA 4, and DNA misfolding.

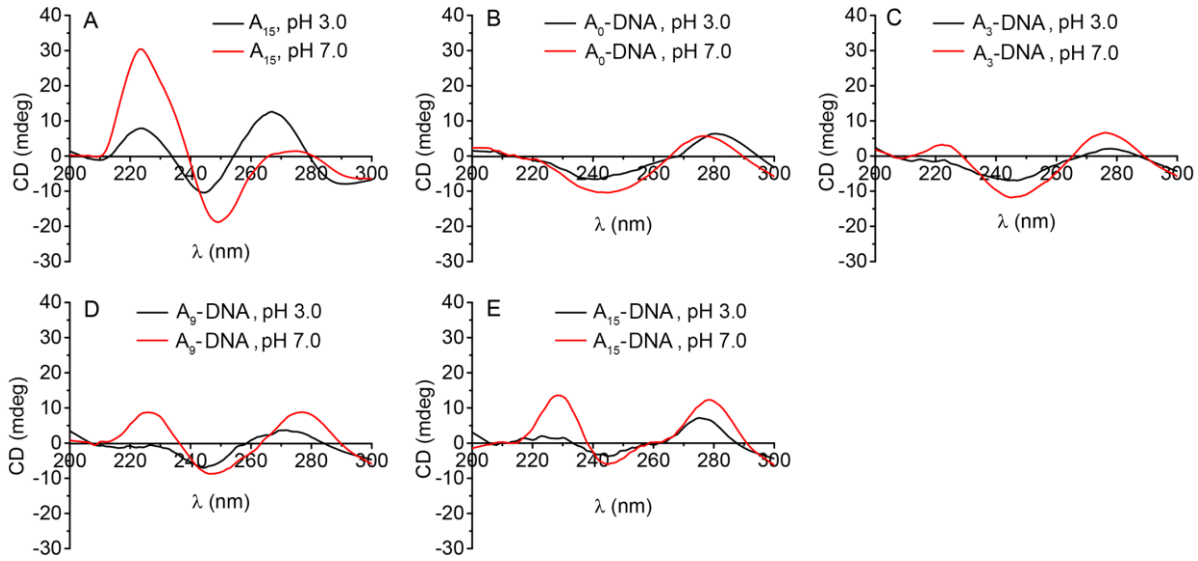

Figure 2.5 CD spectra of 10 μM DNA samples at pH 3.0 and 7.0 adjusted by 10 mM citrate buffer. (A) The A_{15} DNA (DNA 9); (B) A_0-DNA (DNA 1); (C) A_3-DNA (DNA 2); (D) A_9-DNA (DNA 3); and (E) A_{15}-DNA (DNA 4).

2.3.2 CD Spectra of i-motif

Similar to adenine rich DNA, the DNA with poly-C can also form the unique structure (i-motif) at acidic condition. The i-motif has a characteristic CD spectrum with a dominant positive band at 290 nm and a negative band at around 260 nm.[81] Using a series of poly-C containing DNA (DNA 5-8), we measured their CD spectra using the same condition as the poly-A DNA. First, the random DNA was measured to understand the background signal (Figure 2.6 A). Then, the length of poly-C block was increased in the DNA (Figure 2.6 B-D), where the positive peak at 290 nm and the negative peak at 260 became stronger at pH 3.0. This change supports the formation of i-motif structure even when the poly-C DNA is appended with a block of random sequence. The i-motif is a less favorable secondary structure for the DNA conjugation reaction since it contains four DNA strands arranged in an overall anti-parallel manner (Figure 1.4). This may explain the

difficulties associated with forming functional conjugates we previously reported for non-thiolated poly-C containing DNA.[60]

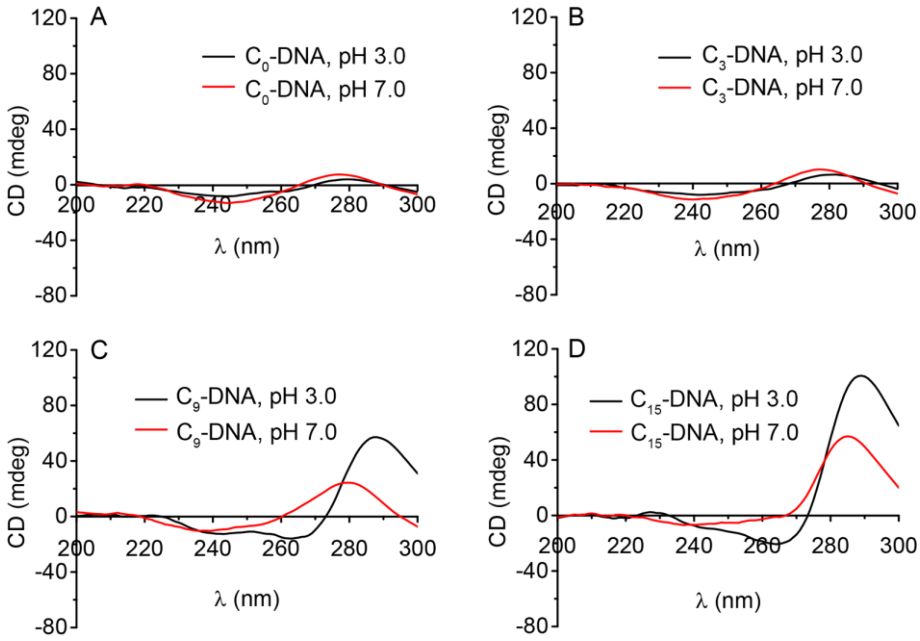

Figure 2.6 CD spectra of 10 µM DNA samples at pH 3.0 and 7.0 in 10 mM citrate buffer. (A) C_0-DNA (DNA 5); (B) C_3-DNA (DNA 6); (C) C_9-DNA (DNA 7); and (D) C_{15}-DNA (DNA 8).

2.3.3 Probing the A-motif by DNA Staining Dyes

Although CD spectroscopy is quite powerful, interpretation of its data is not often straightforward and this is not a very common instrument. Therefore, we also want to develop another method to study parallel poly-A in our system. For this purpose, a number of DNA staining dyes were screened, including SYBR Green I (SGI), ethidium bromide (EB), and thiazole orange (TO).

2.3.3.1 Ethidium Bromide

EB is commonly used to detect DNA or RNA in agarose gel electrophoresis. The fluorescent intensity of EB can be amplified 20 times compared with no DNA.[82] The positive charge of EB can profit it's binding to negatively charged DNA. As shown in Figure 2.7 A, the dye-DNA samples at acidic or neutral condition showed no obvious differences. The fluorescence spectra of EB-A_{30} under 490 nm excitation also showed no selectivity. As a result, EB is not a suitable for probing A-motif.

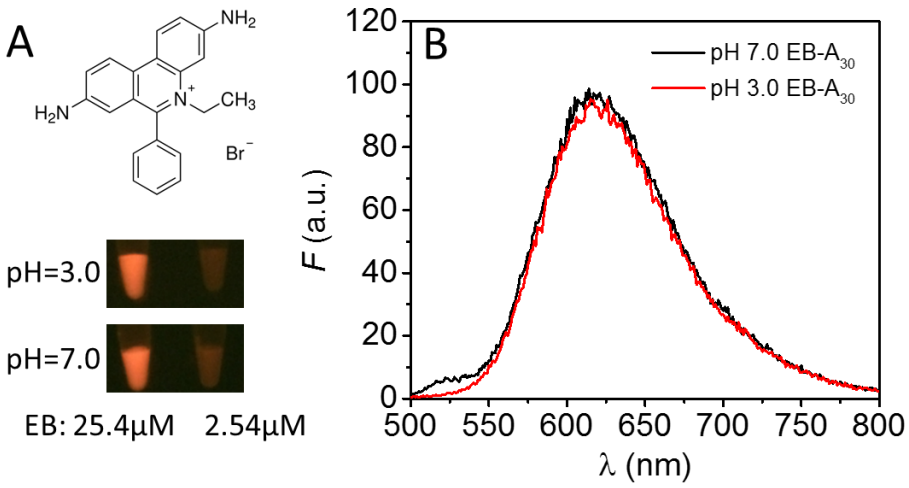

Figure 2.7 (A) Chemical structure of EB and the photos of the DNA samples with different dye concentrations at pH 3.0 and pH 7.0 (under 470 nm light source). (B) Fluorescence emission spectrum of EB-stained A_{30}.

2.3.3.2 SYBR Green I

Compared with EB, SGI (see Figure 2.8 A for structure) is much less toxic. It is an important dye used in the qualitative PCR.[83] As an asymmetrical cyanine, SGI can be excited around 497 nm and the maximal emission peak is near 520 nm. Figure 2.8 B shows that SGI do

not produce a stronger fluorescence for a poly-A DNA at pH 3.0 than that at pH 7.0. We also found that SGI-T_{30} at pH 7.0 also show an emission peak around 540 nm. From the above points, SGI is not a good probing dye for the A-motif.

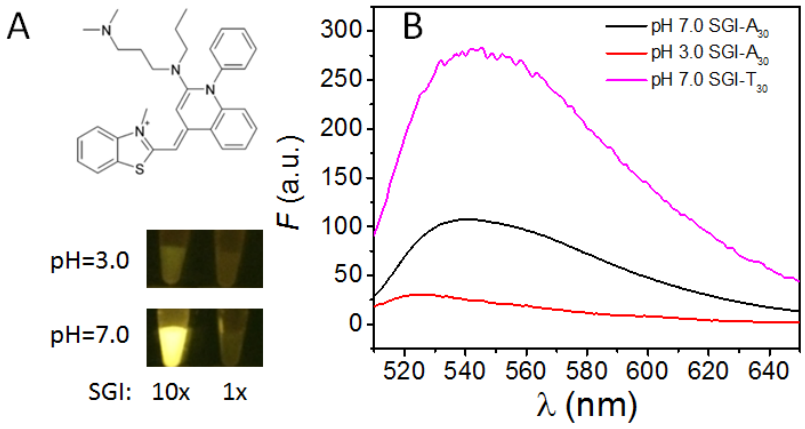

Figure 2.8 (A) Chemical structure of SGI and the photos of the DNA samples with different dye concentrations at pH 3.0 and pH 7.0 (under 470 nm light source). (B) Fluorescence emission spectrum of SGI-stained A_{30}.

2.3.3.3 Thiazole Orange

The affinity between TO and single-strand polypurines is 100 times stronger than that to single-stranded polypyrimidines[84]. In this experiment, TO (see Figure 2.9 A for structure) showed a higher fluorescence with poly-A DNA at pH 3.0 (Figure 2.9 B). This suggests that TO is protected by the poly-A structure at low pH from photobleaching. In contrast, TO is quite insensitive to pH for poly-T or poly-C DNA (Figure 2.9 C & D). Poly-G DNA was not considered here, since they tend to form G-quadruplex and emit very strongly with TO.[85] TO is a useful dye for staining the A-motif if G-quadruplex can be excluded.

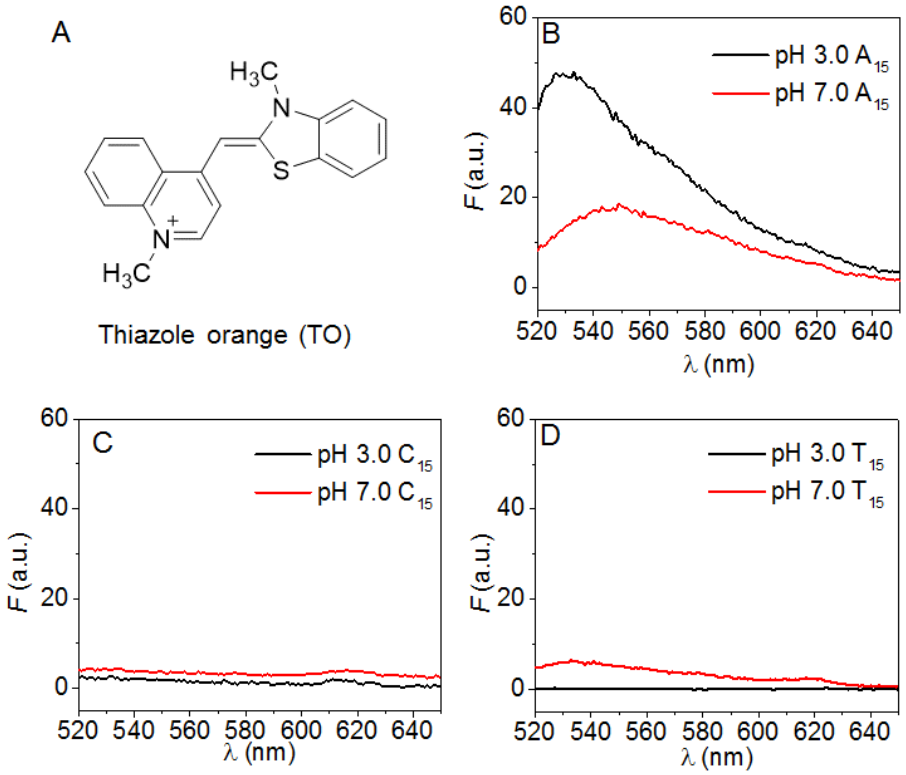

Figure 2.9 (A) The chemical structure of TO. Fluorescence spectra of TO stained (B) A_{15}, (C) C_{15}, and (D) T_{15} DNA at pH 3.0 and pH 7.0.

We then tested the response of TO with DNA 1-4. The DNA with longer poly-A sequence has stronger fluorescent intensity (Figure 2.10 A). This trend correlates well the length of poly-A suggesting the formation of parallel A-motif. At pH 7.0, fluorescent intensity is weak and independent of the length of poly-A (Figure 2.10 B). Therefore, TO staining also supports that the A-motif can form in such DNA.

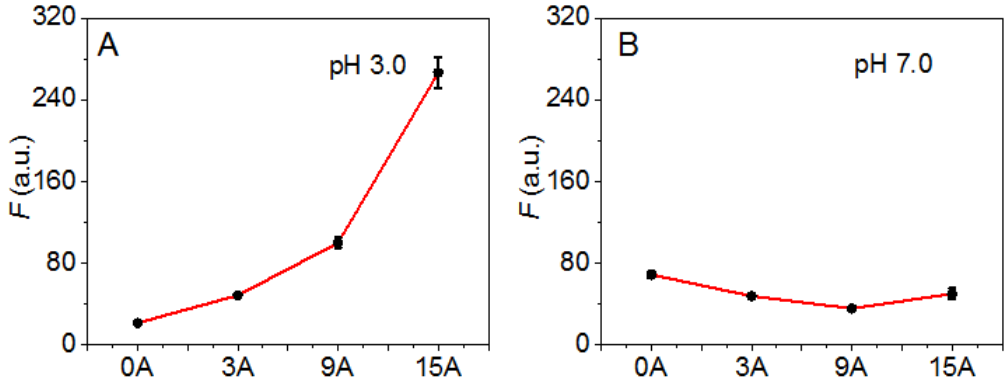

Figure 2.10 The fluorescent intensity of TO stained DNA with different poly-A blocks lengths (A) at pH 3.0 and (B) at pH 7.0. The ratio of DNA and TO molecule is 1:15 in all the samples.

2.4 Conclusions

CD spectroscopy is a powerful way to monitor the folding changes in DNA. From the above experiments, we can make a conclusion that both the A-motif and i-motif structures can be formed even when the poly-A/C DNA is appended with a block of random sequence. The longer poly-A/C blocks in the DNA the easier for the DNA to form higher structures at low pH. The parallel structure of A-motif can still expose the ending active points in the DNA, and these active points will be at the same side of the A-motif. However, the random (functional) sequence in the poly-C DNA will no more in the same side when the i-motif is formed. These differences may bring the totally different performance when poly-A and poly-C DNAs conjugates onto AuNPs.

A few DNA staining dyes were screened for A-motif detection including SYBR green I, ethidium bromide, and thiazole orange. SGI and EB did not produce a stronger fluorescence for a poly-A DNA at pH 3.0 than that at pH 7.0. Only TO showed a higher fluorescence with at pH 3.0. At the same time, the fluorescence of TO stained poly-A DNA is quite stable at low pH for a day,

while the fluorescence of this mixture only can maintain for ~1 h at pH 7.0. The details about the stabilities will be talked in chapter 4. In conclusion, TO is successfully screened as a suitable DNA staining dye for indicating the A-motifs at low pH.

Chapter 3: Attaching A-motif Containing DNA to Gold Nanoparticles

3.1 Introduction

3.1.1 Active Sites in A-motif

Before we discuss the active sites in A-motif, we will mention some basic studies on the interactions between single-stranded DNA (ssDNA) and double-stranded DNA (dsDNA) and AuNPs.[86] Since the DNA bases (as the active points) are responsible for DNA adsorption and the phosphate backbone poses the repulsive barrier, adsorption of ds-DNA and well-folded DNAs with shielded bases are kinetically disfavored. As a result, compared with ssDNA, much lower DNA adsorption densities are obtained for dsDNA (Figure 3.1). Another important work by Kimura-Suda *et al*. indicates that the DNA hybridization energy is weaker compared to chemisorption of DNA by gold.[50]

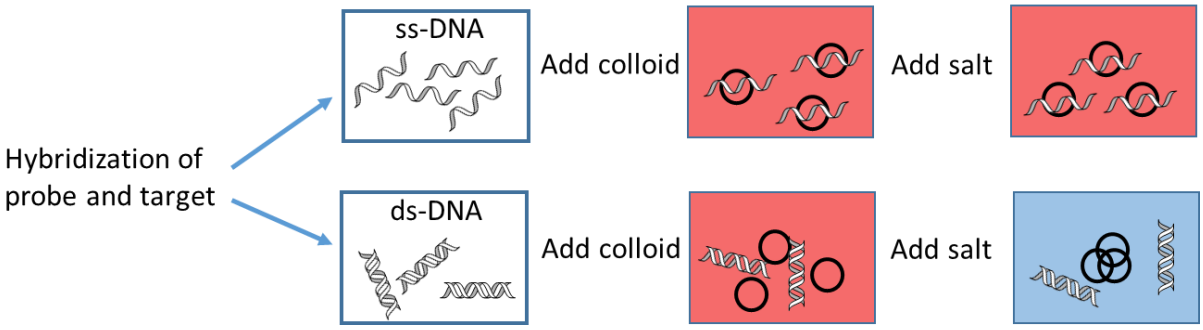

Figure 3.1 Pictorial representation of the colorimetric method for differentiating between single- and double-stranded oligonucleotides. The circles represent colloidal gold nanoparticles.[87]

From the introduction of the interactions between nucleobases and AuNPs in chapter 1, we know that adenine has the strongest affinity energy on gold surface. However, the formation of the A-motif will decrease the chance of the interactions between adenines and gold surface even bury

the active adenines. This should be fine for the thiolated DNA since the A-motif will not bury the thiol group. For non-thiolated DNA, the A-motif may inhibit the poly-A DNA conjugations onto the AuNPs. Yamuna Krishnan *et al.* utilized the molecular dynamic (MD) simulation to draw a 3D structures of single-stranded A_{15} and parallel duplex of A_{15} (A-motif) (Figure 3.2). They found that the ending two/three adenines will not be involved in the AH^+-H^+A pairs. In other words, they are still active for AuNPs.

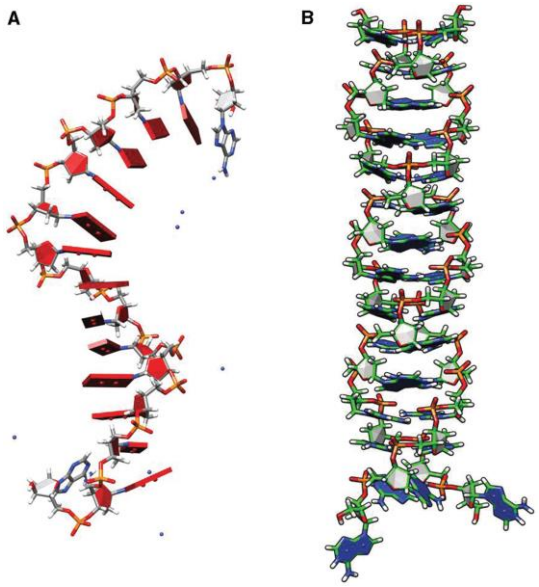

Figure 3.2 (A) Equilibrium snapshot of the single-stranded A_{15} after 20 ns long MD simulating using AMBER revealing highly stacked adenine nucleobases. (B) Instantaneous snapshot of N1-protonated adenosine mediated parallel duplex of A_{15} after 20 ns long MD simulation revealing a Π-helical structure with tilted base.[66] (Reproduced with permission from ref. 66)

3.1.2 Post-Acidification

In the previous studies from our lab, DNA was usually mixed with AuNPs before adding the acidic buffer to lower the pH.[54, 55, 88] This process is named post-acidification. We believe the initial interaction between DNA and AuNPs is helpful for the stabilities of AuNPs because the

adding of the acidic buffer may also introduce salt. With the increasing ionic strength, AuNPs will tend to aggregate. The good qualitative DNA-AuNPs conjugates were synthesized by the post-acidification process.

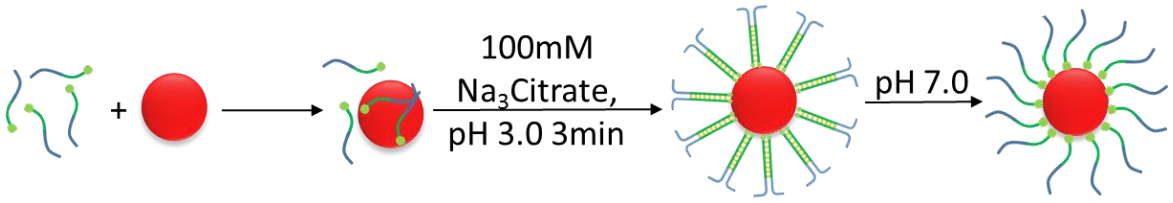

Figure 3.3 The schematic diagram of mixing the DNA and AuNPs before adjusting pH to 3.0.

3.1.3 Pre-Acidification

The special role of the A-motif makes us try to acidify the DNA before they are added into the AuNPs. This process is called pre-acidification. This process will give more time for A-motif formation.

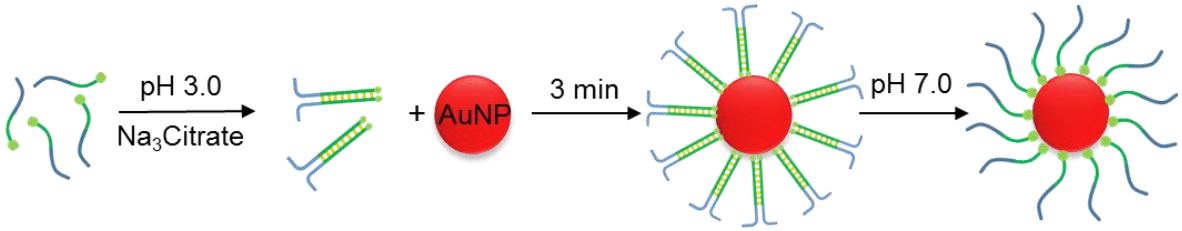

Figure 3.4 The schematic diagram of acidifying the DNA first to form the A-motif before adding AuNPs.

3.1.4 Effect of DNA Length

Fan *et al*. had previously demonstrated that poly-A can serve as an anchoring block for preferential binding with the AuNPs surface. Systematically modulate the lateral spacing and surface density of DNA on AuNPs can be easily realized by simply adjusting the length of the

poly-A block.[89] Normally, the longer poly-A block, the lower density will be achieved by the low-pH method (Figure 3.5).[61]

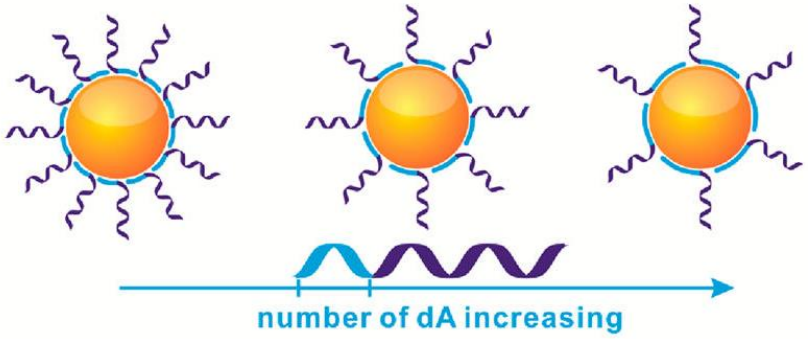

Figure 3.5 Schematic for spatial control on AuNPs by varying the length of poly-A blocks.[62, 90] (Reproduced with permission from ref. 62)

3.1.5 DNA-AuNPs Self-Assembly

DNA modified AuNPs as the biosensors usually work in two ways: (1) hybridization of probes with DNA or RNA targets and (2) association of probes with targets or subunits.[91] One of the most successful examples is colorimetric detection which is physically detectable signal. Herein, an example about DNA-AuNPs biosensor designed for sensing adenosine and cocaine is recited.[32, 92] Figure 3.6 shows the construction of the adenosine sensor. Firstly, AuNPs were separately functionalized with 3′-thiol-modified DNA ($3'Adap_{Au}$) and 5′-thiol-modified DNA ($5'Adap_{Au}$). Then a linker DNA which contains an adenosine aptamer sequence was mixed with the two former DNA-AuNPs conjugates mixture. The aggregation of AuNPs happened when the linker DNA hybridized with both 3′-thiol-modified DNA and 5′-thiol-modified DNA. Aggregated AuNPs showed purple without targets. When the adenosine was added, the linker DNA which is the DNA aptamer for adenosine would bind more strongly with the adenosine molecules. Then, the linking AuNPs will be broken resulting in the recovery of red color. In the UV-vis spectra, the

line in blue is the absorbance spectrum of the aggregation of AuNPs. The nanoparticle aggregates disassembled within 10 seconds of adding adenosine (2 mM) which showed the red curve (Figure 3.6 A). At the same time, the ratio of the absorbance at 522 nm and 700 nm in UV-vis spectrum of the AuNPs increased.

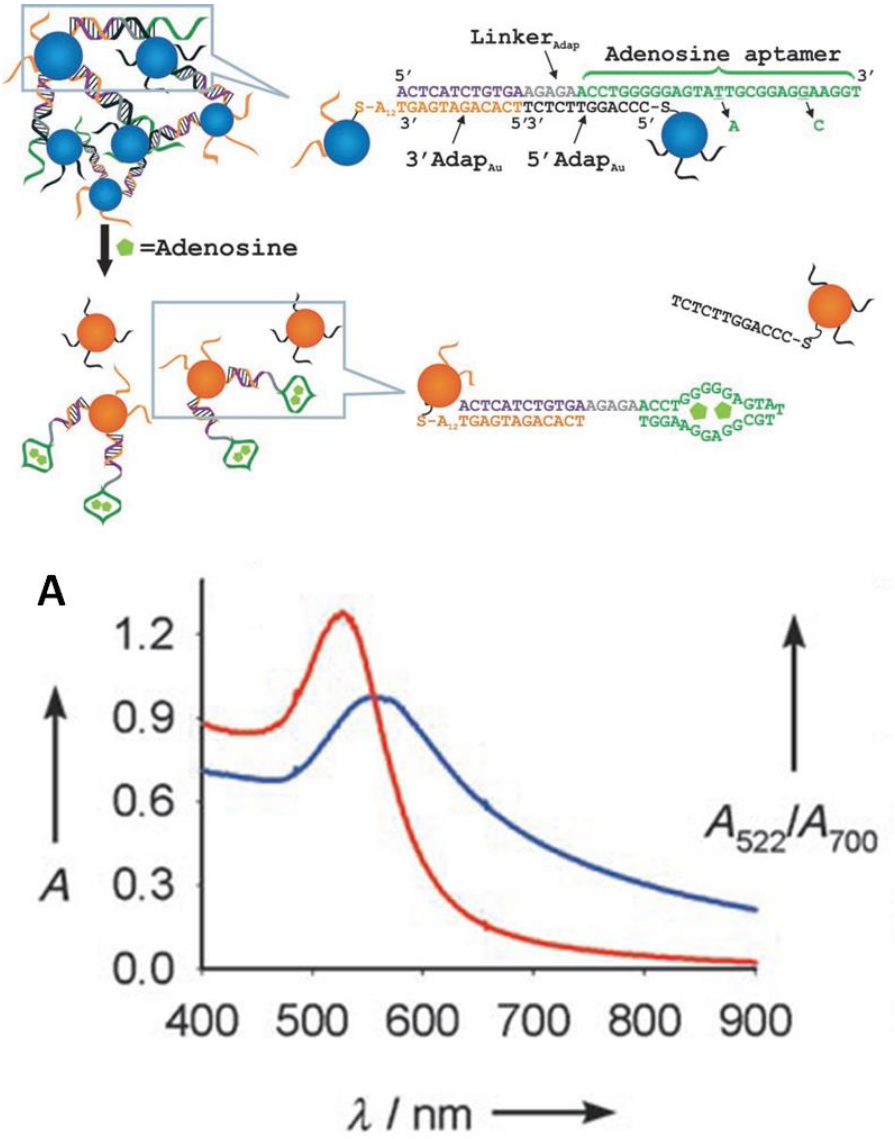

Figure 3.6 Schematic representation of colorimetric detection of adenosine. The DNA sequences are shown in the right side of the figure. (A) Absorbance spectra of the adenosine sensor before

(blue) and 10 seconds after (red) the addition of adenosine (2 mm).[93] (Reproduced with permission from ref. 94)

The goal of this chapter is to study the performance of poly-A DNA (i.e., A-motif) adsorption on citrate-capped AuNPs at low pH, including the DNA adsorption capacity and DNA-AuNP conjugate's functionality. It is also necessary to compare the performances when the A-motif is formed before and after mixing with AuNPs.

3.2 Experimental Section

3.2.1 Chemicals

All the DNA samples were purchased from Integrated DNA Technologies (Coralville, IA). The DNA sequences used are listed in Table 2. DNA 17-21 carries a FAM (carboxyfluorescein) modification on the 3′ -end. $HAuCl_4$ and KCN were from Sigma-Aldrich. Ethanol, sodium hydroxide, and hydrochloric acid were from VWR (Mississauga, ON). Sodium chloride, sodium citrate, and 4-(2-hydroxyethyl) piperazine-1-ethanesulfonate (HEPES) were from Mandel Scientific (Guelph, ON).

Table 3.1 A list of the DNA sequences and modifications used in this work. FAM = carboxyfluorescein.

DNA ID	DNA Names	Sequences and modifications (from 5′ to 3′)
3	A_9-DNA	TTCACAGATGCGTAAAAAAAAA
7	C_9-DNA	TTTCACAGATGCGTCCCCCCCCC
15	SH-DNA	SH-AAAAAAAACCCAGGTTCTCT
16	Linker DNA	ACGCACACACAAAGAGAACCTGGG

17	A_5-FAM	AAAAA-FAM
18	A_{10}-FAM	AAAAAAAAAA-FAM
19	A_{15}-FAM	AAAAAAAAAAAAAAA-FAM
20	A_{30}-FAM	AAAAAAAAAAAAAAA AAAAAAAAAAAAAAA-FAM
21	A_{45}-FAM	AAAAA$(A\sim A)_{35}$AAAAA-FAM

3.2.2 Synthesis of 13 nm AuNPs

Before synthesizing AuNPs, all the glassware and stir bar were soaked in aqua regia for 2 hours. Firstly, add 2 ml of 50 mM $HAuCl_4$ solution into 98 ml of Millipore water in the two-neck flask so that the final $HAuCl_4$ concentration is 1 mM. Then, the flask was heated with refluxing and stirring. When the solution begins to reflux, 10 mL of 38.8 mM sodium citrate was quickly added. Allow the system to reflux for another 20 min. Last, the whole solution was cooled to room temperature. The final concentration of AuNPs were ~10 nM. [94]

3.2.3 UV-vis Characterization

All the samples of the AuNPs for UV-vis spectra (Agilent 8453) were diluted to control the final absorbance intensity is between 0~1. For 13 nm AuNPs, there is a characteristic absorbance peak around 520 nm.[95] The photos of AuNPs were recorded with a digital camera (Canon Powershot SD1200 IS).

3.2.4 DNA Conjugating onto AuNPs

The process of preparing DNA-functionalized AuNPs was the same regardless of the DNA sequences or modification. First, a DNA solution (100 mM, 2 µL) was mixed with 100 µL as-synthesized 13 nm AuNPs. After 3 min incubation, the mixture was adjusted to pH 3.0 by adding

citrate buffer (500 mM, pH 3.0, 2 µL). After 3 min, the mixture was adjusted back to neutral by adding HEPES buffer (500 mM, pH 7.0, 6 µL). Finally, the resulting DNA-functionalized AuNPs were washed with 5 mM HEPES buffer (pH 7.0) for three times by centrifugation at 15,000 rpm for 15 min.

3.2.5 Quantification of the Adsorbed DNA

In our experiments, the DNA adsorption densities were mainly determined by fluorescent signal. AuNPs are excellent fluorescence quenchers, yielding a large change in fluorescence signal upon fluorescently labeled DNA (FAM-DNA) adsorption/desorption. For FAM-labeled DNA, the quantification was performed by determining the fluorescence intensity of the diluted KCN-treated sample with a plate reader (Infinite F200 Pro, Tecan). The adsorption capacities of DNAs in our experiments will be given by comparing the fluorescence intensity of samples with a standard curve following literature reported procedures (Figure 3.7 A).[96] For non-FAM-labeled DNAs, after dissolving the AuNPs cores with KCN solution, a DNA staining dye will be added to provide a fluorescent signal when the dyes combine with DNAs (Figure 3.7 B).

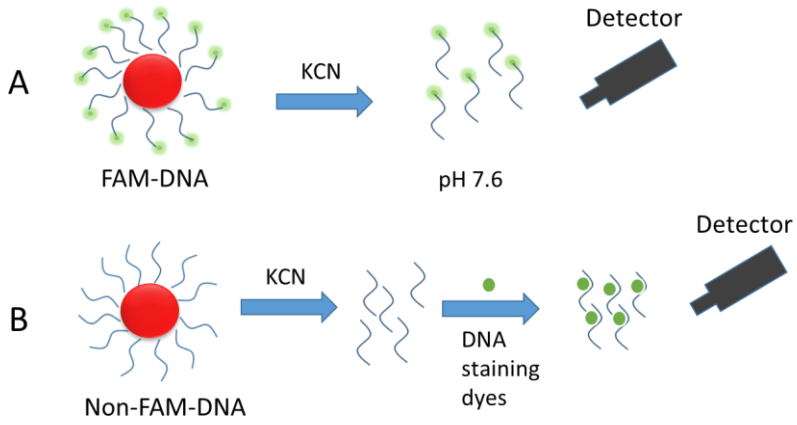

Figure 3.7 (A) Determination of the adsorption density of FAM-labeled DNA. (B) Utilizing DNA staining dyes to detect the adsorption density of non-FAM-labeled DNA.

3.3 Results and Discussion

3.3.1 AuNPs Binding Capacity

The DNA adsorption density on AuNPs is a key factor for the performance of the DNA-AuNPs conjugates. The capacity of the AuNPs were studied by absorbing different poly-A oligonucleotides whose lengths vary from 5 to 45 at low pH. As shown in Figure 3.8, the longer length of the poly-A sequence, the lower DNA adsorption density was obtained. This trend is consistent with the poly-A adsorption density at neutral pH.[62]

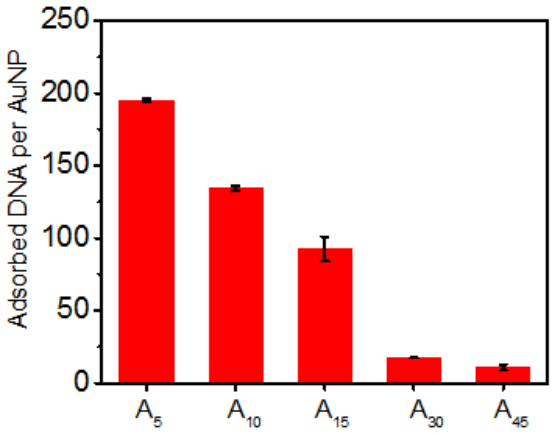

Figure 3.8 Poly-A DNA adsorption density as a function of the length of poly-A.

3.3.2 Order of mixing

So far, the protocol has been mixing the DNA and AuNPs first without adjusting pH, followed by adding pH 3.0 citrate buffer to a final concentration of 10 mM. We call it post-acidification. We want to test the effect of acidifying DNA before mixing it with AuNPs (i.e. pre-acidification). This may give more time for A-motif formation.

We first tested two non-thiolated DNA. The A_{10} and A_{15} DNAs were chosen since this length range is often used as a spacer. In one group, DNA was mixed with AuNPs before adjusting the pH to 3.0 (Figure 3.9 A). In another group, DNA was first incubated at pH 3.0 before adding AuNPs (Figure 3.9 B). We further measured the loaded DNA density on AuNPs (Figure 3.9 C). For both A_{10} and A_{15}, a higher density was achieved by the post-acidification method. The DNA density trend is also consistent with the stability measurement (details will be shown in the next chapter). It might be that during pre-acidification, a stable A-motif can form, resulting in most adenine nucleotides buried in the duplex and thus weaker interaction with the AuNP surface.[97] Since these DNAs were non-thiolated and they require the adenine-AuNP interaction for adsorption, a lower stability was observed for the pre-acidification method.

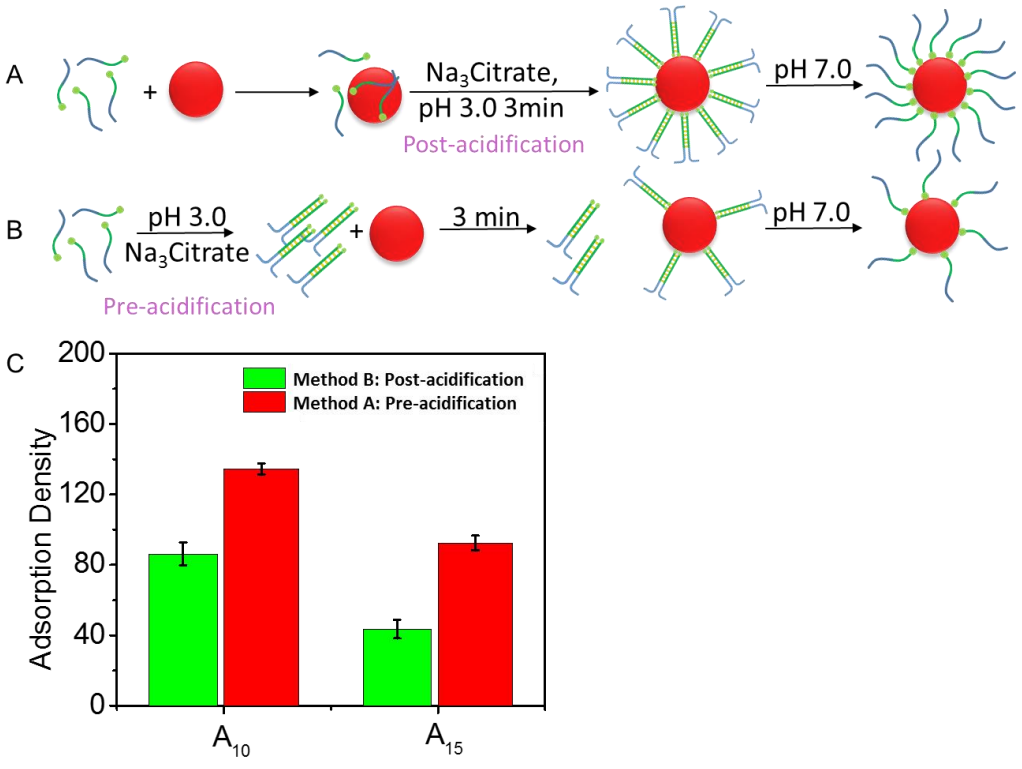

Figure 3.9 The schematic diagram of (A) mixing the DNA and AuNP before adjusting pH to 3 and (B) acidifying the DNA first to form the A-motif before adding AuNPs. The methods in (A)

and (B) are called post- and pre-acidification, respectively. The final composition of these two samples are the same and only the order of mixing is different. (C) The DNA adsorption density of A_{10} and A_{15} on AuNPs using these two methods.

3.3.3 Functionality of DNA-AuNPs

The polarity of DNA is particularly important for DNA-directed assembly. In this thesis, we use DNA with two blocks: a poly-A block (i.e., anchor sequence) and a functional block (i.e., sequence for hybridization). To test the functionality of our DNA-AuNPs conjugates, we modify AuNPs with another thiolated DNA with a nine-adenine block. Then, the poly-A DNA modified AuNPs were mixed with the thiolated DNA modified AuNPs. After adding linker DNA strands, which are complementary to the two DNAs (except the nine-adenine spacer) adsorbed on AuNPs, to the mixture of the two conjugates, purple aggregates happened (Figure 3.10 A). The process of AuNP aggregation is reversible by changing temperature. When the temperature is higher than the melting T, AuNPs solution will return to red. In the UV-vis spectra, no peak shifts were observed before and after the AuNPs were modified with the DNAs (Figure 3.10 B). When AuNPs are assembled by linker DNA, there were shifts in the surface plasmon band that can be monitored using UV−vis spectroscopy (Figure 3.10 C). The similar experiment was repeated on the poly-C DNA modified AuNPs, and the same result was given.

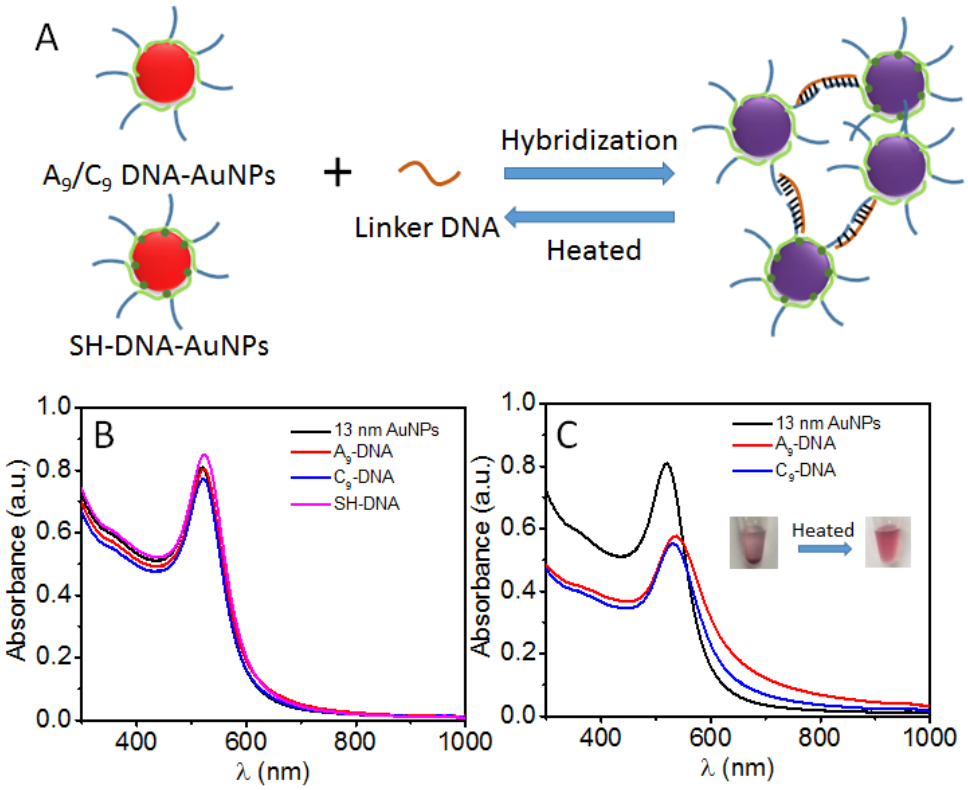

Figure 3.10 (A) The scheme of the chrmetric detection based on the DNA directed AuNPs self-assembly. (B) UV-vis spectra of bare AuNPs and poly-A/C and thiolated DNA modified AuNPs. (C) UV−vis spectra and photographic images (inset) for the DNA directed AuNPs self-assembly.

3.4 Conclusions

DNA adsorption density is one important reference value to evaluate a DNA-AuNP conjugate. On one hand, when the conjugates were designed as biosensors, the higher DNA adsorption density always meant better stability, faster response speed, and higher sensitivity. To avoid the poly-A DNA laying down and wrapping around the AuNP, pre-acidification seems to be helpful. The result is that the traditional post-acidification is favorable in DNA adsorption. This might be the formation of A-motif before mixing DNA with AuNPs does avoid more adenine bases in one ss-DNA interact with the gold surface, however, A-motif also decrease the chance of

interacting between DNA and gold surface. On the other hand, too high DNA adsorption density may lead to limited space for further DNA hybridization. The functionality experiment results support that functional DNA-AuNP conjugate was successfully synthesized with the help of A-motif.

Chapter 4: Stability of DNA at Low pH

4.1 Introduction

4.1.1 DNA Stability at Low pH

The stability of the DNA at low pH is the main concern during the low-pH conjugating process. The acid can catalyze the depurination of DNA.[98] Depurination, the process of releasing purine bases from nucleic acids by the hydrolysis of N-glycosidic bonds, has attracted considerable attention since it is closely related to the damage of nucleic acids. In the poly-A DNA, N7 atom of the adenine will be protonated at the low pH. This results in the formation of the monoprotonated intermediate, which leads to the transition of the charge of the oxygen atom in the deoxyribose. Then another proton will attack the N3 atom, leading adenine to fall off (Figure 4.1). The position where the adenine/guanine is absent is called apurinic (AP) sites. The depurination could affect the normal properties of the DNA, including hybridization, mutagenesis, carcinogenesis and cellular aging.[99-102]

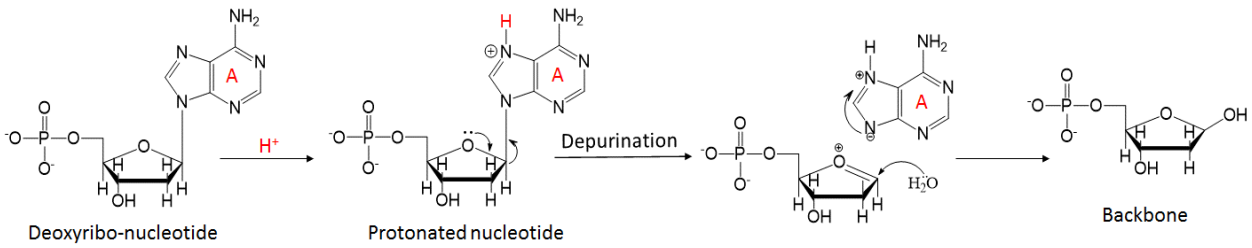

Figure 4.1 The schematic diagram of the depurination reaction and subsequent DNA cleavage by protonation mechanism. At low pH, poly-purine DNAs such as poly-A and poly-G are unstable due to this reason.

4.1.2 DNA Stabilized AuNPs

In our experiments, the citrate-capped 13 nm AuNPs were used. The bare 13 nm AuNPs are very sensitive to the salt. Aggregation (show blue or purple color) will happen when the concentration of salt (i.e., NaCl) increases (Figure 4.2 A). The effect of the bivalent salt (e.g., Mg^{2+} and Ca^{2+}) even is more obvious. The resistance to the salt induced aggregation of AuNPs can be improved by surface modification. A well-established system has been applied to stabilize AuNPs including surfactants, protein, polymers, ionic liquid, and DNA.[49, 103-106] Herein, we focused on the DNA stabilized AuNPs. On one hand, the modification of ssDNA on the AuNPs can noticeably improve the AuNP's colloidal stability, due to the electrostatic repulsion force between two negatively charged DNA strands (Figure 4.2 B). On the other hand, the dsDNA buries the nucleobases, leading to the weak interaction between ds-DNA and AuNP. As a result, the protection on AuNPs from dsDNA is too weak to avoid the aggregation (Figure 4.2 C). The stability of the DNA-AuNP conjugates can be used to estimate the DNAs' adsorption density and their spatial arrangements. At the same time, it is important for us to understand how salt and stable AuNPs are coexisting during the salt-aging method. As mentioned above in chapter 1, salt can screen the negative charge of DNA and AuNP. It is helpful for DNA adsorption. In salt-aging method, the concentration of salt is increased in multiple steps to avoid aggregation. Therefore, the salt-aging method always need over 12 hours even a day.

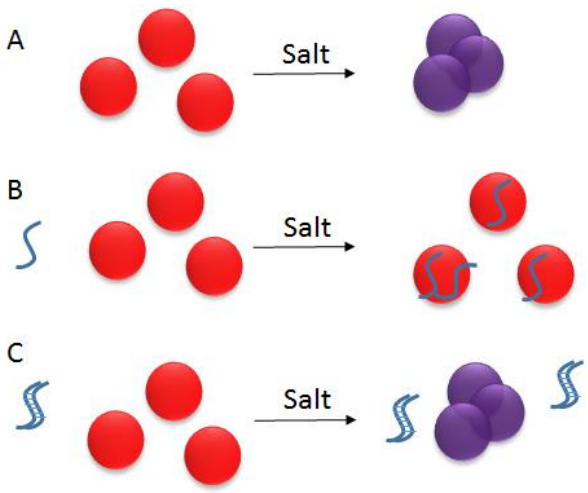

Figure 4.2 Salt effects on the stabilities of the AuNPs. (A) A low salt concentration can induce bare AuNP aggregation. (B) Adsorption of ss-DNA can protect AuNPs from salt induced aggregation. (C) Adsorption of ds-DNA is kinetically slow and AuNPs are not protected.

4.1.3 Gel Electrophoresis

15% Polyacrylamide gel electrophoresis (PAGE) is a commonly used technique to separate DNAs with different lengths by electrophoretic mobility.[107-109] Detection and collection of various lengths of DNAs can be achieved at the same time. In this chapter, PAGE gel was used to study the cleavage degrees of DNAs at different pHs, and the stability of poly-A DNA at pH 3.0 as a function of time. The A-motif DNA may be formed with the poly-A DNA during the low-pH DNA adsorption method. It is also possible that poly-A DNA might be cleaved via the depurination reaction at pH below 3.5 if incubated for a long time. PAGE gel is a simple way to prove whether the poly-A DNA will be cleaved into shorter fragments.

Far more than this, gel electrophoresis also can be carried out with DNA-AuNP conjugates. The Gel percentage, buffers, voltage, and time are needed to be considered to separate the DNA-AuNP conjugates with different DNA adsorption densities. The position of the DNA-AuNP

conjugates can be easily seen with the naked eyes. Figure 4.3 shows the migration rate of the conjugates decreases as the length of poly-A increases. In Figure 4.3, the left picture is taken under digital gel imaging systems, and the right picture is the photographic image taken under daylight. According to the migration rate, a conclusion can be draw that adsorption density of DNA strands are decreased with the increase of poly-A block length.

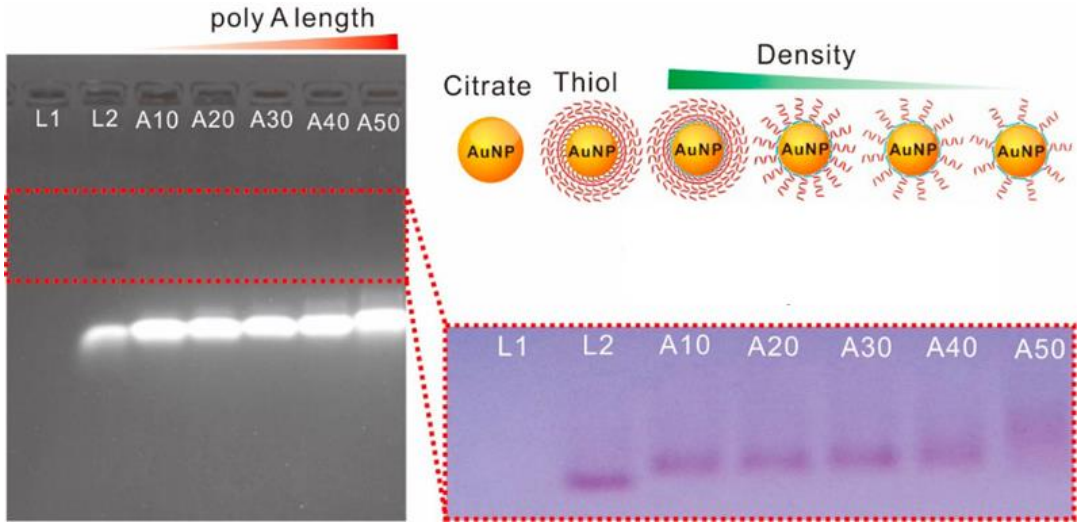

Figure 4.3 Agarose gel electrophoresis images showing the increased migration rate with the increase of polyA length. L1: Citrate-modified AuNPs, L2: Thiolated-DNA-AuNPs conjugates.[90] (Reproduced with permission from ref. 91)

The goal of this chapter is to study the stability of the poly-A DNA modified AuNPs under various concentrations of NaCl salt. This can reflect the binding strength between poly-A DNA and AuNPs. Due to the potential DNA damage caused by acidic environment, the stability of the home poly-A and poly-G oligonucleotides will be discussed. A stable DNA is essential for functional DNA-AuNP conjugate.

4.2 Experimental Section

4.2.1 Chemicals

All the DNA samples were purchased from Integrated DNA Technologies (Coralville, IA). The DNA sequences used are listed in Table 3. SYBR Green I (SGI) was from Invitrogen (Carlsbad, CA). $HAuCl_4$ were from Sigma-Aldrich. Ethanol, sodium hydroxide, and hydrochloric acid were from VWR (Mississauga, ON). Sodium chloride, sodium citrate, and 4-(2-hydroxyethyl) piperazine-1-ethanesulfonate (HEPES) were from Mandel Scientific (Guelph, ON).

Table 4.1 A list of the DNA sequences and modifications used in this work. FAM = carboxyfluorescein.

DNA ID	DNA Names	Sequences and modifications (from 5′ to 3′)
9	A_{15}	AAAAAAAAAAAAAAA
10	T_{15}	TTTTTTTTTTTTTTT
11	G_{15}	GGGGGGGGGGGGGGG
12	C_{15}	CCCCCCCCCCCCCCC
22	A_{10}	AAAAAAAAAA
23	A_{30}	AAAAAAAAAAAAAAA AAAAAAAAAAAAAAA
24	5′SH-A_9-DNA	SH-AAAAAAAAACCCAGGTTCTCT
25	3′SH-A_9-DNA	TCACAGATGCGTAAAAAAAAA-SH
26	FAM-DNA	FAM-ACGCATCTGTGA

4.2.2 DNA-AuNPs Stability

To test the colloidal stability of AuNPs, 5 M NaCl was add to 100 µL DNA-functionalized AuNPs to achieve a final NaCl concentration of 200, 400, and 600 mM. The color of the resulting AuNPs was documented using a digital camera.

4.2.3 Gel Electrophoresis

Poly-A DNA (1 μM) was incubated at different pH values for various amount of time. Then all the samples were adjusted to neutral pH before analyzed by 15% denaturing polyacrylamide gel electrophoresis (dPAGE). To test the possibility of forming apurinic (AP) sites, the A_{15} DNA (1 μM) was incubated under different pH's for 12 h. Then the samples were adjusted to neutral pH with 500 mM HEPES buffer, followed by adding a final of 1 μM T_{15} DNA for hybridization. After hybridization, SGI dye was added to stain the duplex DNA (ratio of DNA: SGI was 1:15). The same process was performed with the G_{15} DNA, except that C_{15} was added for hybridization. The final SGI fluorescence was measured by exciting at 485 nm and the emission was quantified at 535 nm.

4.3 Results and Discussion

4.3.1 The Stabilities of the DNA-AuNP conjugates in Salt Solution

Individually dispersed AuNPs are red, while their color changes to blue/purple upon salt-induced aggregation. By simply observing the color, the colloidal stability of AuNPs can be judged. For both A_{10} and A_{15}, a better stability was achieved with the post-acidification method (Figure 4.4, the first two groups). To further understand it, we next used a few thiolated DNA each containing a A_9 spacer (DNA 24, 25). In this case, both methods yielded a similarly high stability (Figure 4.4, the last two groups). With a thiol group, its interaction with the AuNP surface dominates the adenine base interaction. As a result, the A-motif conformation is not that important. Overall, post-acidification appears to be the optimal method for non-thiolated DNA, while for thiolated DNA, either method should work.

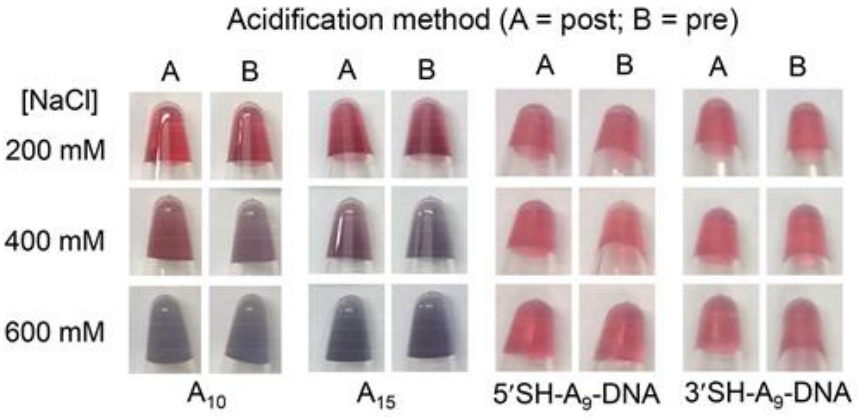

Figure 4.4 The stability of the A_{10}, A_{15}, and two thiolated DNA with a A_9 spacer conjugated AuNPs assayed in different concentrations of NaCl using the methods in (A) and (B), respectively.

4.3.2 DNA Stability at Low pH.

At low pH, DNA may undergo depurination and then cleavage.[110] Therefore, DNA is vulnerable at the adenine and guanine sites in acids. Since poly-A DNA is studied here, its stability at low pH is important to understand. To test this, we used FAM-labeled A_{15} and a random FAM-DNA (DNA 26). These DNAs were incubated at various pH from 1.0 to 7.0 for 1 h and then analyzed with gel electrophoresis (Figure 4.5 A&B). Neither the random DNA nor poly-A DNA was cleaved at pH 3.0 or even pH 1.0. Next, we incubated the FAM-A_{15} at pH 3.0 for up to 24 h, and still no degradation was observed (Figure 4.5 C).

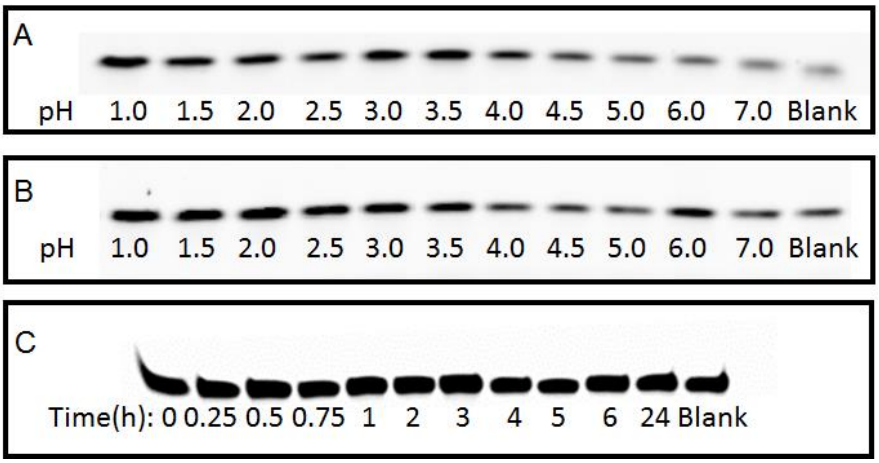

Figure 4.5 Gel electrophoresis micrographs showing the stability of (A) A_{15} and (B) a random DNA (DNA 26) incubated at different pH values for 1 h, and (C) A_{15} incubated at pH 3.0 for various amount of time.

The lack of cleavage products, however, may not fully exclude the possibility of apurinic sites (e.g. depurinated without cleavage). To test this, we then designed a hybridization experiment. We incubated the A_{15} DNA in pH 1.0-7.0 buffers for 12 h. Then all the samples were brought to neutral pH and mixed with the same concentration of T_{15} to form duplex. Finally, SGI was added to stain the DNA, and all the samples showed a similar fluorescence intensity (Figure 4.6 A). This result suggests that the A_{15} is still functional for hybridization and depurination is unlikely to happen. In contrast, the G_{15} DNA has lost or lowered its integrity at pH 3.0 based on its hybridization with C_{15} and then staining (Figure 4.6 B). The result is consistent with the longer half-life of A_{30} (97 h) than G_{18} (24 h) at pH 1.6. In the case of pH 2.5 at 37 °C, the half-life of A_{30} is 230 h.[111] For our conjugation method at pH 3, the stability of poly-A DNA is sufficient. However, we still need to be careful of the guanine nucleotides to keep them stable.

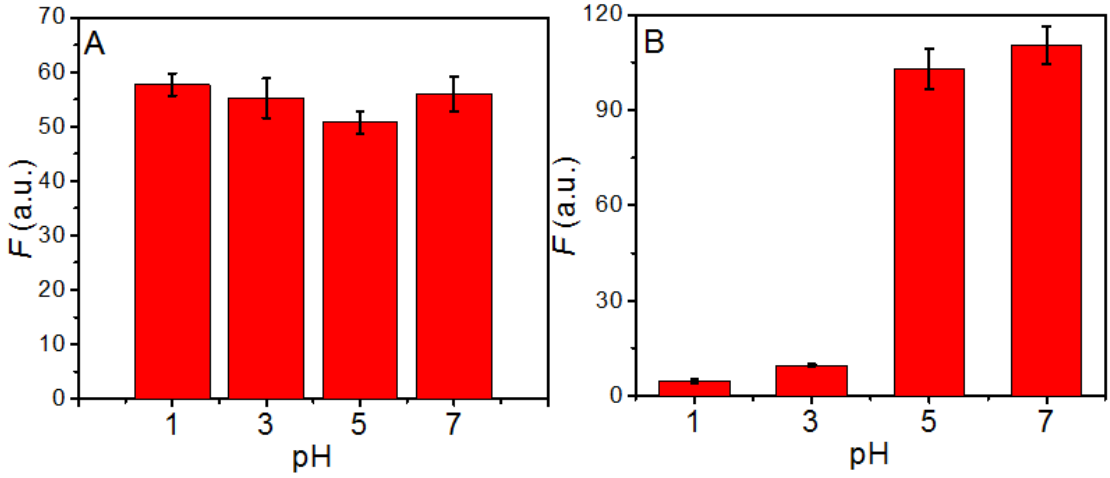

Figure 4.6 The fluorescence intensity of (A) A_{15} and (B) G_{15} after incubation at various pH for 12 h and then hybridized with T_{15} or G_{15} at neutral pH to form duplex and finally stained with SGI.

4.3.3 Stabilities of the Dye-DNA Conjugates

The high stability of the dye-DNA conjugate is basic for the possibility of applying the dye in detecting DNA.[112] In this part, the stability of the dye-DNA conjugate was studied as a function of time. We screened three common dyes to indicate A-motif structure. TO not only has a unique response for the poly-A oligonucleotides at low pH, but also show a better stability at pH 3.0 than pH 7.0. Figure 4.7 shows that the fluorescence of TO stained poly-A DNA is quite stable at low pH for a day, while the fluorescence of this mixture only can maintain for ~1 h at pH 7.0.

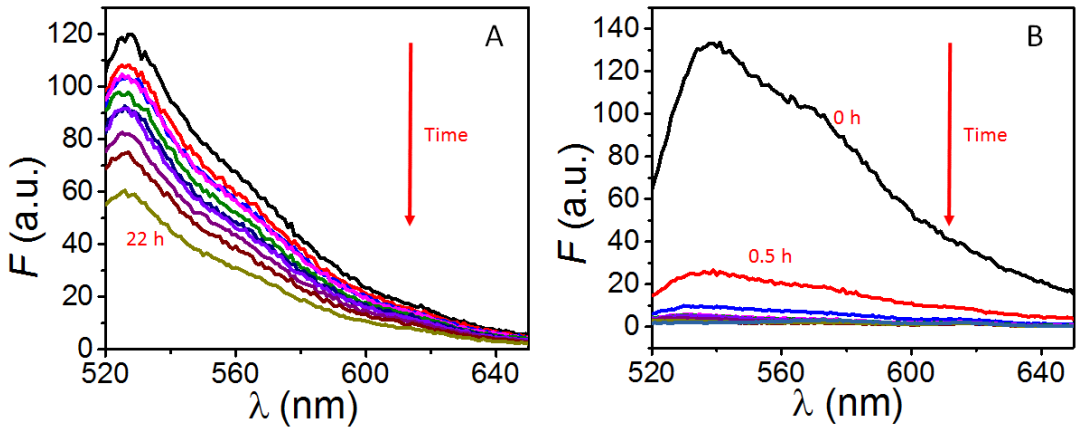

Figure 4.7 The stability of TO-A_{30} conjugates at (A) pH 3.0 and (B) pH 7.0.

4.4 Conclusions

In this chapter, the stabilities of DNA-AuNP conjugates in salt solution was firstly discussed. The ability of bearing higher NaCl concentration (i.e., ionic strength) reflect higher DNA adsorption density. The stability results of A_{10} and A_{15} supported that traditional post-acidification is better, which is consistent with conclusion in chapter 3. However, for thiolated DNA, both post-acidification and pre-acidification work. Next, the stability of homo poly-A DNA at different pH, especially pH 3.0, is mainly studied. From the PAGE gel results, no cleavage was observed in A_{15} even under pH 1.0 for 24 h. This indicates the stability of the poly-A DNA phosphate backbone and sugar ring. In order to rule out the possibility of AP sites, a hybridization experiment was designed and G_{15} was introduced as a control. After incubating A_{15} and G_{15} under a series pH conditions, A_{15} and G_{15} respectively hybridized with their complementary DNA. The hybridization bonds involve the adenine and guanine bases, and enhanced fluorescence will happen when the SGI dye molecules combine with the hybridization bonds. The fluorescent results

of SGI-A_{15} and SGI-G_{15} is consistent with the half-life (A_{30} 97 h and G_{18} 24 h) in the reference.[111] Overall, the stability of poly-A DNA is sufficient for the low-pH modifying method.

Chapter 5: Conclusions

In this thesis, I confirmed the role of the parallel poly-A duplex at low pH in assisting the DNA conjugation reaction to AuNPs. This method works for both thiolated and non-thiolated DNA, as long as they contain a block of poly-A segment. For thiolated DNA, a high DNA density can be easily rationalized. At low pH, both thermodynamic and kinetic effects are favorable for achieving a high density of DNA with the intended DNA conformation. There is no need for the thiol group to displace adsorbed DNA bases. Therefore, this low pH method works very well for thiolated DNA with a poly-A block. For non-thiolated DNA, the kinetic factor dominates initially. Although adenine can displace other bases especially thymine, it is not as efficient as thiol displacing DNA bases.[50] Forming the A-motif at low pH can also help non-thiolated DNA to be adsorbed in the intended conformation.

The formation of such A-motifs in DNA sequences containing a block of adenine (the rest are random sequences) is supported by CD spectroscopy. We further screened a few DNA staining dyes showing that TO can selectively detect the A-motif at low pH. While the previous understanding was focused on electrostatic interactions, this work shows the unique role of DNA conformation. The order of mixing DNA and AuNPs and pH adjustment have also been optimized. For non-thiolated DNA, the optimal attachment is achieved by mixing poly-A DNA and AuNPs at neutral pH followed by pH adjustment. For thiolated DNA, adjusting pH either before or after mixing DNA with AuNPs can work. For the same conformational reasons, poly-C DNAs forming the i-motif are less favorable for the low pH method. Finally, we confirmed that poly-A DNA is very stable under the acidic pH conditions for the AuNP conjugation reaction, while the stability of poly-G DNA is relatively lower due to the depurination reaction. This work has provided new insights into the reaction between DNA and AuNPs, and it will facilitate related research in

biosensor development and nanotechnology. While the current discussion is made with AuNPs, the formation of A-motif at low pH is independent of gold. Bearing this in mind, it is also possible to design poly-A DNA sequences at low pH for interacting with other surfaces.

This study has also implication on DNA sequence design for the bioconjugation reaction. In retrospect, it was quite lucky that our lab initially followed Mirkin's sequence design to involve a block of poly-A sequence as a spacer.[54] After observing the interesting effect of low pH, it was initially attributed to a simple electrostatic model. In this work, we emphasized also on the effect of DNA conformation, which allowed us to explain the difference between poly-A and poly-C spacer,[60] and also the adsorption of non-thiolated DNA. Now that the importance of the parallel poly-A is confirmed, we can intentionally design sequences to contain poly-A instead of poly-C. Using a poly-T spacer might work well with the salt-aging method but it is unlikely to be a good choice for the low-pH method since thymine cannot be protonated. Poly-G may also fold to complex quadruplex structures and cannot be protonated either unless pH is lower than 2, where guanine nucleotide is expected to suffer from depurination and cleavage. In addition to poly-A, some other special sequences may also form parallel duplexes. This however require two different strands of carefully designed sequences.[113] Their contribution to DNA adsorption to AuNPs is less easy to generalize.

References

1. Liu, B.; Liu, J., DNA Adsorption by Magnetic Iron Oxide Nanoparticles and Its Application for Arsenate Detection. *Chem. Commun.* **2014,** 50, 8568-70.

2. Liu, B.; Liu, J., Accelerating Peroxidase Mimicking Nanozymes Using DNA. *Nanoscale* **2015,** 7, 13831-5.

3. Liu, Q.; Pu, Z.; Asiri, A. M.; Al-Youbi, A. O.; Sun, X., Polydopamine Nanospheres: A Biopolymer-Based Fluorescent Sensing Platform for DNA Detection. *Sens. Actuators, B* **2014,** 191, 567-571.

4. Clark, S. J.; Smallwood, S. A.; Lee, H. J.; Krueger, F.; Reik, W.; Kelsey, G., Genome-Wide Base-Resolution Mapping of DNA Methylation in Single Cells Using Single-Cell Bisulfite Sequencing (Scbs-Seq). *Nat. Protocols* **2017,** 12, 534-547.

5. Hu, R.; Zhang, X.; Zhao, Z.; Zhu, G.; Chen, T.; Fu, T.; Tan, W., DNA Nanoflowers for Multiplexed Cellular Imaging and Traceable Targeted Drug Delivery. *Angew. Chem., Int. Ed.* **2014,** 53, 5821-5826.

6. Wang, C.; Tao, Y.; Pu, F.; Ren, J.; Qu, X., pH-Responsive DNA Assembly Regulated through A-Motif. *Soft Matter* **2011,** 7, 10574-10580.

7. Bloomfield, V. A.; Crothers, D. M.; Tinoco, I., *Nucleic Acids: Structures, Properties, and Functions*. Sterling Publishing Company: 2000.

8. Yang, Y.; Li, C.; Yin, L.; Liu, M.; Wang, Z.; Shu, Y.; Li, G., Enhanced Charge Transfer by Gold Nanoparticle at DNA Modified Electrode and Its Application to Label-Free DNA Detection. *ACS Appl. Mater. Interfaces* **2014,** 6, 7579-7584.

9. Lu, C.; Liu, Y.; Ying, Y.; Liu, J., Comparison of Mos2, Ws2, and Graphene Oxide for DNA Adsorption and Sensing. *Langmuir* **2017,** 33, 630-637.

10. Lu, C.; Huang, P.-J. J.; Liu, B.; Ying, Y.; Liu, J., Comparison of Graphene Oxide and Reduced Graphene Oxide for DNA Adsorption and Sensing. *Langmuir* **2016,** 32, 10776-10783.

11. Pautler, R.; Kelly, E. Y.; Huang, P. J.; Cao, J.; Liu, B.; Liu, J., Attaching DNA to Nanoceria: Regulating Oxidase Activity and Fluorescence Quenching. *ACS Appl. Mater. Interfaces* **2013,** 5, 6820-5.

12. Morris, W.; Briley, W. E.; Auyeung, E.; Cabezas, M. D.; Mirkin, C. A., Nucleic Acid–Metal Organic Framework (MOF) Nanoparticle Conjugates. *J. Am. Chem. Soc.* **2014,** 136, 7261-7264.

13. Cai, B.; Wang, S.; Huang, L.; Ning, Y.; Zhang, Z.; Zhang, G.-J., Ultrasensitive Label-Free Detection of PNA–DNA Hybridization by Reduced Graphene Oxide Field-Effect Transistor Biosensor. *ACS Nano* **2014,** 8, 2632-2638.

14. Su, S.; Fan, J.; Xue, B.; Yuwen, L.; Liu, X.; Pan, D.; Fan, C.; Wang, L., DNA-Conjugated Quantum Dot Nanoprobe for High-Sensitivity Fluorescent Detection of DNA and Micro-RNA. *ACS Appl. Mater. Interfaces* **2014,** 6, 1152-1157.

15. Choi, J.; Majima, T., Conformational Changes of Non-B DNA. *Chem. Soc. Rev.* **2011,** 40, 5893-5909.

16. Kim, S.; Choi, J.; Majima, T., Self-Assembly of Polydeoxyadenylic Acid Studied at the Single-Molecule Level. *J. Phys. Chem. B* **2011,** 115, 15399-405.

17. Safaee, N.; Noronha, A. M.; Rodionov, D.; Kozlov, G.; Wilds, C. J.; Sheldrick, G. M.; Gehring, K., Structure of the Parallel Duplex of Poly(A) RNA: Evaluation of a 50 Year-Old Prediction. *Angew. Chem., Int. Ed.* **2013,** 52, 10370-3.

18. Westhof, E.; Sundaralingam, M., X-Ray-Structure of a Cytidylyl-3',5'-Adenosine-Proflavine Complex: A Self-Paired Parallel-Chain Double Helical Dimer with an Intercalated Acridine Dye. *Proc. Natl. Acad. Sci. U. S. A.* **1980,** 77, 1852-1856.

19. Liu, B.; Liu, J., Comprehensive Screen of Metal Oxide Nanoparticles for DNA Adsorption, Fluorescence Quenching, and Anion Discrimination. *ACS Appl. Mater. Interfaces* **2015,** 7, 24833-8.

20. Huang, Z.; Liu, B.; Liu, J., Parallel Polyadenine Duplex Formation at Low pH Facilitates DNA Conjugation onto Gold Nanoparticles. *Langmuir* **2016**.

21. Li, X.; Peng, Y.; Ren, J.; Qu, X., Carboxyl-Modified Single-Walled Carbon Nanotubes Selectively Induce Human Telomeric i-motif Formation. *Proc. Natl. Acad. Sci. U. S. A.* **2006,** 103, 19658-19663.

22. Zhang, X.; Liu, B.; Dave, N.; Servos, M. R.; Liu, J., Instantaneous Attachment of an Ultrahigh Density of Nonthiolated DNA to Gold Nanoparticles and Its Applications. *Langmuir* **2012,** 28, 17053-60.

23. Sau, T. K.; Rogach, A. L.; Jäckel, F.; Klar, T. A.; Feldmann, J., Properties and Applications of Colloidal Nonspherical Noble Metal Nanoparticles. *Adv. Mater.* **2010,** 22, 1805-1825.

24. Njoki, P. N.; Lim, I. I. S.; Mott, D.; Park, H.-Y.; Khan, B.; Mishra, S.; Sujakumar, R.; Luo, J.; Zhong, C.-J., Size Correlation of Optical and Spectroscopic Properties for Gold Nanoparticles. *J. Phys. Chem. C* **2007,** 111, 14664-14669.

25. Samanta, A.; Medintz, I. L., Nanoparticles and DNA - a Powerful and Growing Functional Combination in Bionanotechnology. *Nanoscale* **2016,** 8, 9037-9095.

26. Ghosh, P.; Han, G.; De, M.; Kim, C. K.; Rotello, V. M., Gold Nanoparticles in Delivery Applications. *Adv. Drug Delivery Rev.* **2008,** 60, 1307-1315.

27. Zhu, Q.-L.; Li, J.; Xu, Q., Immobilizing Metal Nanoparticles to Metal–Organic Frameworks with Size and Location Control for Optimizing Catalytic Performance. *J. Am. Chem. Soc.* **2013,** 135, 10210-10213.

28. Lin, L.-S.; Cong, Z.-X.; Cao, J.-B.; Ke, K.-M.; Peng, Q.-L.; Gao, J.; Yang, H.-H.; Liu, G.; Chen, X., Multifunctional Fe_3O_4@Polydopamine Core–Shell Nanocomposites for Intracellular Mrna Detection and Imaging-Guided Photothermal Therapy. *ACS Nano* **2014,** 8, 3876-3883.

29. Wu, L.; Ma, C.; Zheng, X.; Liu, H.; Yu, J., Paper-Based Electrochemiluminescence Origami Device for Protein Detection Using Assembled Cascade DNA–Carbon Dots Nanotags Based on Rolling Circle Amplification. *Biosensors and Bioelectronics* **2015,** 68, 413-420.

30. Liu, B.; Kelly, E. Y.; Liu, J., Cation-Size-Dependent DNA Adsorption Kinetics and Packing Density on Gold Nanoparticles: An Opposite Trend. *Langmuir* **2014,** 30, 13228-34.

31. Ma, L.; Liu, B.; Huang, P.-J. J.; Zhang, X.; Liu, J., DNA Adsorption by ZnO Nanoparticles near Its Solubility Limit: Implications for DNA Fluorescence Quenching and Dnazyme Activity Assays. *Langmuir* **2016,** 32, 5672-5680.

32. Zhao, W.; Chiuman, W.; Brook, M. A.; Li, Y., Simple and Rapid Colorimetric Biosensors Based on DNA Aptamer and Noncrosslinking Gold Nanoparticle Aggregation. *ChemBioChem* **2007,** 8, 727-731.

33. Rosi, N. L.; Mirkin, C. A., Nanostructures in Biodiagnostics. *Chem. Rev.* **2005,** 105, 1547-1562.

34. Liu, J.; Cao, Z.; Lu, Y., Functional Nucleic Acid Sensors. *Chem. Rev.* **2009,** 109, 1948-1998.

35. Zhao, W.; Brook, M. A.; Li, Y., Design of Gold Nanoparticle-Based Colorimetric Biosensing Assays. *ChemBioChem* **2008,** 9, 2363-2371.

36. Song, S.; Qin, Y.; He, Y.; Huang, Q.; Fan, C.; Chen, H.-Y., Functional Nanoprobes for Ultrasensitive Detection of Biomolecules. *Chem. Soc. Rev.* **2010,** 39, 4234-4243.

37. Wilner, O. I.; Willner, I., Functionalized DNA Nanostructures. *Chem. Rev.* **2012,** 112, 2528-2556.

38. Wang, H.; Yang, R.; Yang, L.; Tan, W., Nucleic Acid Conjugated Nanomaterials for Enhanced Molecular Recognition. *ACS Nano* **2009,** 3, 2451-2460.

39. Giljohann, D. A.; Seferos, D. S.; Daniel, W. L.; Massich, M. D.; Patel, P. C.; Mirkin, C. A., Gold Nanoparticles for Biology and Medicine. *Angew. Chem., Int. Ed.* **2010,** 49, 3280-3294.

40. Torabi, S.-F.; Lu, Y., Functional DNA Nanomaterials for Sensing and Imaging in Living Cells. *Curr. Opin. Biotechnol.* **2014,** 28, 88-95.

41. Pinheiro, A. V.; Han, D.; Shih, W. M.; Yan, H., Challenges and Opportunities for Structural DNA Nanotechnology. *Nat. Nanotechnol.* **2011,** 6, 763-772.

42. Liu, W.; Tagawa, M.; Xin, H. L.; Wang, T.; Emamy, H.; Li, H.; Yager, K. G.; Starr, F. W.; Tkachenko, A. V.; Gang, O., Diamond Family of Nanoparticle Superlattices. *Science* **2016,** 351, 582-586.

43. Jones, M. R.; Seeman, N. C.; Mirkin, C. A., Programmable Materials and the Nature of the DNA Bond. *Science* **2015,** 347.

44. Tan, L. H.; Xing, H.; Lu, Y., DNA as a Powerful Tool for Morphology Control, Spatial Positioning, and Dynamic Assembly of Nanoparticles. *Acc. Chem. Res.* **2014,** 47, 1881-1890.

45. Koo, K. M.; Sina, A. A. I.; Carrascosa, L. G.; Shiddiky, M. J. A.; Trau, M., DNA-Bare Gold Affinity Interactions: Mechanism and Applications in Biosensing. *Anal. Methods* **2015,** 7, 7042-7054.

46. Liu, J., Adsorption of DNA onto Gold Nanoparticles and Graphene Oxide: Surface Science and Applications. *Phys. Chem. Chem. Phys.* **2012,** 14, 10485-96.

47. Herne, T. M.; Tarlov, M. J., Characterization of DNA Probes Immobilized on Gold Surfaces. *J. Am. Chem. Soc.* **1997,** 119, 8916-8920.

48. Lang, N. J.; Liu, B.; Zhang, X.; Liu, J., Dissecting Colloidal Stabilization Factors in Crowded Polymer Solutions by Forming Self-Assembled Monolayers on Gold Nanoparticles. *Langmuir* **2013,** 29, 6018-24.

49. Storhoff, J. J.; Elghanian, R.; Mirkin, C. A.; Letsinger, R. L., Sequence-Dependent Stability of DNA-Modified Gold Nanoparticles. *Langmuir* **2002,** 18, 6666-6670.

50. Kimura-Suda, H.; Petrovykh, D. Y.; Tarlov, M. J.; Whitman, L. J., Base-Dependent Competitive Adsorption of Single-Stranded DNA on Gold. *J. Am. Chem. Soc.* **2003,** 125, 9014-9015.

51. Demers, L. M.; Mirkin, C. A.; Mucic, R. C.; Reynolds, R. A.; Letsinger, R. L.; Elghanian, R.; Viswanadham, G., A Fluorescence-Based Method for Determining the Surface Coverage and Hybridization Efficiency of Thiol-Capped Oligonucleotides Bound to Gold Thin Films and Nanoparticles. *Anal. Chem.* **2000,** 72, 5535-5541.

52. Cutler, J. I.; Auyeung, E.; Mirkin, C. A., Spherical Nucleic Acids. *J. Am. Chem. Soc.* **2012,** 134, 1376-1391.

53. Zhang, X.; Servos, M. R.; Liu, J., Surface Science of DNA Adsorption onto Citrate-Capped Gold Nanoparticles. *Langmuir* **2012,** 28, 3896-902.

54. Zhang, X.; Servos, M. R.; Liu, J., Instantaneous and Quantitative Functionalization of Gold Nanoparticles with Thiolated DNA Using a pH-Assisted and Surfactant-Free Route. *J. Am. Chem. Soc.* **2012,** 134, 7266-9.

55. Zhang, X.; Gouriye, T.; Göeken, K.; Servos, M. R.; Gill, R.; Liu, J., Toward Fast and Quantitative Modification of Large Gold Nanoparticles by Thiolated DNA: Scaling of Nanoscale Forces, Kinetics, and the Need for Thiol Reduction. *J. Phys. Chem. C* **2013,** 117, 15677-15684.

56. Ohta, S.; Glancy, D.; Chan, W. C. W., DNA-Controlled Dynamic Colloidal Nanoparticle Systems for Mediating Cellular Interaction. *Science* **2016,** 351, 841-845.

57. Shi, D.; Song, C.; Jiang, Q.; Wang, Z.-G.; Ding, B., A Facile and Efficient Method to Modify Gold Nanorods with Thiolated DNA at a Low pH Value. *Chem. Commun.* **2013,** 49, 2533-2535.

58. Zhang, X.; Servos, M. R.; Liu, J., Fast pH-Assisted Functionalization of Silver Nanoparticles with Monothiolated DNA. *Chem. Commun.* **2012,** 48, 10114-6.

59. Zhou, W.; Ding, J.; Liu, J., A Platinum Shell for Ultraslow Ligand Exchange: Unmodified DNA Adsorbing More Stably on Platinum Than Thiol and Dithiol on Gold. *Chem. Commun.* **2015,** 51, 12084-7.

60. Zhang, X.; Liu, B.; Servos, M. R.; Liu, J., Polarity Control for Nonthiolated DNA Adsorption onto Gold Nanoparticles. *Langmuir* **2013,** 29, 6091-8.

61. Opdahl, A.; Petrovykh, D. Y.; Kimura-Suda, H.; Tarlov, M. J.; Whitman, L. J., Independent Control of Grafting Density and Conformation of Single-Stranded DNA Brushes. *Proc. Natl. Acad. Sci. U. S. A.* **2007,** 104, 9-14.

62. Pei, H.; Li, F.; Wan, Y.; Wei, M.; Liu, H.; Su, Y.; Chen, N.; Huang, Q.; Fan, C., Designed Diblock Oligonucleotide for the Synthesis of Spatially Isolated and Highly Hybridizable Functionalization of DNA–Gold Nanoparticle Nanoconjugates. *J. Am. Chem. Soc.* **2012,** 134, 11876-11879.

63. Tan, L. H.; Yue, Y.; Satyavolu, N. S. R.; Ali, A. S.; Wang, Z.; Wu, Y.; Lu, Y., Mechanistic Insight into DNA-Guided Control of Nanoparticle Morphologies. *J. Am. Chem. Soc.* **2015,** 137, 14456-14464.

64. Shen, J.; Xu, L.; Wang, C.; Pei, H.; Tai, R.; Song, S.; Huang, Q.; Fan, C.; Chen, G., Dynamic and Quantitative Control of the DNA-Mediated Growth of Gold Plasmonic Nanostructures. *Angew. Chem., Int. Ed.* **2014,** 53, 8338-8342.

65. Song, T.; Tang, L.; Tan, L. H.; Wang, X.; Satyavolu, N. S. R.; Xing, H.; Wang, Z.; Li, J.; Liang, H.; Lu, Y., DNA-Encoded Tuning of Geometric and Plasmonic Properties of Nanoparticles Growing from Gold Nanorod Seeds. *Angew. Chem., Int. Ed.* **2015,** 54, 8114-8118.

66. Chakraborty, S.; Sharma, S.; Maiti, P. K.; Krishnan, Y., The Poly dA Helix: A New Structural Motif for High Performance DNA-Based Molecular Switches. *Nucleic Acids Res.* **2009,** 37, 2810-7.

67. Safaee, N.; Noronha, A. M.; Rodionov, D.; Kozlov, G.; Wilds, C. J.; Sheldrick, G. M.; Gehring, K., Structure of the Parallel Duplex of Poly(A) RNA: Evaluation of a 50 Year-Old Prediction. *Angew. Chem., Int. Ed.* **2013,** 52, 10370-10373.

68. Luzio, J. P.; Pryor, P. R.; Bright, N. A., Lysosomes: Fusion and Function. *Nat. Rev. Mol. Cell Biol.* **2007,** 8, 622-632.

69. Saha, S.; Chakraborty, K.; Krishnan, Y., Tunable, Colorimetric DNA-Based pH Sensors Mediated by A-Motif Formation. *Chem. Commun.* **2012,** 48, 2513-5.

70. Vorlíčková, M.; Kejnovská, I.; Bednářová, K.; Renčiuk, D.; Kypr, J., Circular Dichroism Spectroscopy of DNA: From Duplexes to Quadruplexes. *Chirality* **2012,** 24, 691-698.

71. Holm, A. I. S.; Nielsen, L. M.; Hoffmann, S. V.; Nielsen, S. B., Vacuum-Ultraviolet Circular Dichroism Spectroscopy of DNA: A Valuable Tool to Elucidate Topology and Electronic Coupling in DNA. *Phys. Chem. Chem. Phys.* **2010,** 12, 9581-9596.

72. Chen, C.; Li, M.; Xing, Y.; Li, Y.; Joedecke, C.-C.; Jin, J.; Yang, Z.; Liu, D., Study of pH-Induced Folding and Unfolding Kinetics of the DNA i-Motif by Stopped-Flow Circular Dichroism. *Langmuir* **2012,** 28, 17743-17748.

73. Khimji, I.; Doan, K.; Bruggeman, K.; Huang, P. J.; Vajha, P.; Liu, J., Extraction of DNA Staining Dyes from DNA Using Hydrophobic Ionic Liquids. *Chem. Commun.* **2013,** 49, 4537-9.

74. Yan, X.; Grace, W. K.; Yoshida, T. M.; Habbersett, R. C.; Velappan, N.; Jett, J. H.; Keller, R. A.; Marrone, B. L., Characteristics of Different Nucleic Acid Staining Dyes for DNA Fragment Sizing by Flow Cytometry. *Anal. Chem.* **1999,** 71, 5470-5480.

75. Gaylord, B. S.; Heeger, A. J.; Bazan, G. C., DNA Hybridization Detection with Water-Soluble Conjugated Polymers and Chromophore-Labeled Single-Stranded DNA. *J. Am. Chem. Soc.* **2003,** 125, 896-900.

76. Xu, B. C.; Wu, X. Y.; Yeow, E. K. L.; Shao, F. W., A Single Thiazole Orange Molecule Forms an Exciplex in a DNA i-motif. *Chem. Commun.* **2014,** 50, 6402-6405.

77. Jissy, A.; Konar, S.; Datta, A., Molecular Switching Behavior in Isosteric DNA Base Pairs. *ChemPhysChem* **2013,** 14, 1219-1226.

78. Holm, A. I. S.; Munksgaard Nielsen, L.; Vrønning Hoffmann, S.; Brøndsted Nielsen, S., On the Formation of the Double Helix between Adenine Single Strands at Acidic pH from Synchrotron Radiation Circular Dichroism Experiments. *Biopolymers* **2012,** 97, 550-557.

79. Zheng, B.; Cheng, S.; Liu, W.; Lam, M. H.; Liang, H., A Simple Colorimetric pH Alarm Constructed from DNA-Gold Nanoparticles. *Anal. Chim. Acta* **2012,** 741, 106-13.

80. Saha, S.; Bhatia, D.; Krishnan, Y., pH-Toggled DNA Architectures: Reversible Assembly of Three-Way Junctions into Extended 1D Architectures through a-Motif Formation. *Small* **2010,** 6, 1288-92.

81. Kypr, J.; Kejnovská, I.; Renčiuk, D.; Vorlíčková, M., Circular Dichroism and Conformational Polymorphism of DNA. *Nucleic Acids Res.* **2009,** 37, 1713-1725.

82. Parish, C. R., Fluorescent Dyes for Lymphocyte Migration and Proliferation Studies. *Immunology And Cell Biology* **1999,** 77, 499-508.

83. Yeung, S. S. W.; Lee, T. M. H.; Hsing, I. M., Electrochemistry-Based Real-Time Pcr on a Microchip. *Anal. Chem.* **2008,** 80, 363-368.

84. Nygren, J.; Svanvik, N.; Kubista, M., The Interactions between the Fluorescent Dye Thiazole Orange and DNA. *Biopolymers* **1998,** 46, 39-51.

85. Lubitz, I.; Zikich, D.; Kotlyar, A., Specific High-Affinity Binding of Thiazole Orange to Triplex and G-Quadruplex DNA. *Biochemistry* **2010,** 49, 3567-3574.

86. Li; Rothberg, L. J., Label-Free Colorimetric Detection of Specific Sequences in Genomic DNA Amplified by the Polymerase Chain Reaction. *J. Am. Chem. Soc.* **2004,** 126, 10958-10961.

87. Li, H.; Rothberg, L., Colorimetric Detection of DNA Sequences Based on Electrostatic Interactions with Unmodified Gold Nanoparticles. *Proc. Natl. Acad. Sci. U. S. A.* **2004,** 101, 14036-14039.

88. Zhou, W.; Wang, F.; Ding, J.; Liu, J., Tandem Phosphorothioate Modifications for DNA Adsorption Strength and Polarity Control on Gold Nanoparticles. *ACS Appl. Mater. Interfaces* **2014,** 6, 14795-14800.

89. Yao, G.; Pei, H.; Li, J.; Zhao, Y.; Zhu, D.; Zhang, Y.; Lin, Y.; Huang, Q.; Fan, C., Clicking DNA to Gold Nanoparticles: Poly-Adenine-Mediated Formation of Monovalent DNA-Gold Nanoparticle Conjugates with Nearly Quantitative Yield. *NPG Asia Mater* **2015,** 7, e159.

90. Chen, L.; Chao, J.; Qu, X.; Zhang, H.; Zhu, D.; Su, S.; Aldalbahi, A.; Wang, L.; Pei, H., Probing Cellular Molecules with Polya-Based Engineered Aptamer Nanobeacon. *ACS Appl. Mater. Interfaces* **2017**.

91. Chao, J.; Zhu, D.; Zhang, Y. N.; Wang, L. H.; Fan, C. H., DNA Nanotechnology-Enabled Biosensors. *Biosens. Bioelectron.* **2016,** 76, 68-79.

92. Sassolas, A.; Leca-Bouvier, B. D.; Blum, L. J., DNA Biosensors and Microarrays. *Chem. Rev.* **2008,** 108, 109-139.

93. Liu, J.; Lu, Y., Fast Colorimetric Sensing of Adenosine and Cocaine Based on a General Sensor Design Involving Aptamers and Nanoparticles. *Angew. Chem., Int. Ed.* **2006,** 45, 90-94.

94. Liu, J.; Lu, Y., Preparation of Aptamer-Linked Gold Nanoparticle Purple Aggregates for Colorimetric Sensing of Analytes. *Nat. Protoc.* **2006,** 1, 246-252.

95. Haiss, W.; Thanh, N. T. K.; Aveyard, J.; Fernig, D. G., Determination of Size and Concentration of Gold Nanoparticles from UV−Vis Spectra. *Anal. Chem.* **2007,** 79, 4215-4221.

96. Hurst, S. J.; Lytton-Jean, A. K. R.; Mirkin, C. A., Maximizing DNA Loading on a Range of Gold Nanoparticle Sizes. *Anal. Chem* **2006,** 78, 8313-8318.

97. Bano, F.; Sluysmans, D.; Wislez, A.; Duwez, A.-S., Unraveling the Complexity of the Interactions of DNA Nucleotides with Gold by Single Molecule Force Spectroscopy. *Nanoscale* **2015,** 7, 19528-19533.

98. Oakeley, E. J., DNA Methylation Analysis: A Review of Current Methodologies. *Pharmacol. Ther.* **1999,** 84, 389-400.

99. Raizis, A. M.; Schmitt, F.; Jost, J. P., A Bisulfite Method of 5-Methylcytosine Mapping That Minimizes Template Degradation. *Anal. Biochem.* **1995,** 226, 161-166.

100. Schaaper, R. M.; Loeb, L. A., Depurination Causes Mutations in Sos-Induced Cells. *Proc. Natl. Acad. Sci. U. S. A.* **1981,** 78, 1773-1777.

101. Lindahl, T., Instability and Decay of the Primary Structure of DNA. *Nature* **1993,** 362, 709-715.

102. Lindahl, T.; Andersson, A., Rate of Chain Breakage at Apurinic Sites in Double-Stranded Deoxyribonucleic Acid. *Biochemistry* **1972,** 11, 3618-3623.

103. Zhang, H.; Cui, H., Synthesis and Characterization of Functionalized Ionic Liquid-Stabilized Metal (Gold and Platinum) Nanoparticles and Metal Nanoparticle/Carbon Nanotube Hybrids. *Langmuir* **2009,** 25, 2604-2612.

104. Ishii, T.; Otsuka, H.; Kataoka, K.; Nagasaki, Y., Preparation of Functionally Pegylated Gold Nanoparticles with Narrow Distribution through Autoreduction of Auric Cation by A-Biotinyl-Peg-Block-[Poly(2-(N,N-Dimethylamino)Ethyl Methacrylate)]. *Langmuir* **2004,** 20, 561-564.

105. Johnson, S. R.; Evans, S. D.; Brydson, R., Influence of a Terminal Functionality on the Physical Properties of Surfactant-Stabilized Gold Nanoparticles. *Langmuir* **1998,** 14, 6639-6647.

106. Housni, A.; Ahmed, M.; Liu, S.; Narain, R., Monodisperse Protein Stabilized Gold Nanoparticles Via a Simple Photochemical Process. *J. Phys. Chem. C* **2008,** 112, 12282-12290.

107. Southern, E. M., Detection of Specific Sequences among DNA Fragments Separated by Gel Electrophoresis. *J. Mol. Biol.* **1975,** 98, 503-517.

108. Ganguly, A.; Rock, M. J.; Prockop, D. J., Conformation-Sensitive Gel Electrophoresis for Rapid Detection of Single-Base Differences in Double-Stranded Pcr Products and DNA Fragments: Evidence for Solvent-Induced Bends in DNA Heteroduplexes. *Proc. Natl. Acad. Sci. U. S. A.* **1993,** 90, 10325-10329.

109. Sheffield, V. C.; Cox, D. R.; Lerman, L. S.; Myers, R. M., Attachment of a 40-Base-Pair G + C-Rich Sequence (Gc-Clamp) to Genomic DNA Fragments by the Polymerase Chain Reaction Results in Improved Detection of Single-Base Changes. *Proc. Natl. Acad. Sci. U. S. A.* **1989,** 86, 232-236.

110. Suzuki, T.; Ohsumi, S.; Makino, K., Mechanistic Studies on Depurination and Apurinic Site Chain Breakage in Oligodeoxyribonucleotides. *Nucleic Acids Res.* **1994,** 22, 4997-5003.

111. An, R.; Jia, Y.; Wan, B.; Zhang, Y.; Dong, P.; Li, J.; Liang, X., Non-Enzymatic Depurination of Nucleic Acids: Factors and Mechanisms. *PLoS One* **2014,** 9, e115950.

112. Benson, S. C.; Mathies, R. A.; Glazer, A. N., Heterodimeric DNA-Binding Dyes Designed for Energy Transfer: Stability and Applications of the DNA Complexes. *Nucleic Acids Res.* **1993,** 21, 5720-5726.

113. Parvathy, V. R.; Bhaumik, S. R.; Chary, K. V. R.; Govil, G.; Liu, K.; Howard, F. B.; Miles, H. T., Nmr Structure of a Parallel-Stranded DNA Duplex at Atomic Resolution. *Nucleic Acids Res.* **2002,** 30, 1500-1511.